Abstract

Observations of polarization, incident angle and arriving direction of auroral hiss were carried out at Syowa Station during the period of 1967 to 1970. The present paper consists of two parts. In Part I, we describe the equipment used for the measurement of polarization, incident and azimuthal angles and show the obtained results. The direction finding (DF) system used is based on the analysis of Lissajous' figures of electric and magnetic fields displayed on cathode ray tubes. The individual polarization of the received signal is also measured. Moreover, auroral hiss is decomposed into right- and left-handed polarized components, and these two components are continuously recorded.

From the discussion of the observed results, it is found that auroral hiss has propagated downward in the azimuthal direction from a not so broad range around the magnetic meridian plane and its incident angle is also not so large. Additionally, in most cases, auroral hiss is known to consist of wave components downcoming from multiple directions in the azimuthal and incident planes. The DF system used was found to be effective in a few cases of isolated and sharp auroral hiss. However, this system should be re-examined because it is, strictly speaking, useful only for monochromatic waves, while the auroral hiss seems to have a noise-like nature. Therefore, a new DF system applying the correlation method is being planned to study, with more accuracy, the azimuthal and incident angles of noisy signals such as auroral hiss.

The polarization of auroral hiss received on the ground seems to be almost right-handed circular, at VLF and LF, which is theoretically confirmed by the full wave calculation of the polarization using the realistic model of the auroral ionosphere. On the other hand, the observed polarization of ELF hiss is slightly right-handed circular, which can be reasonably accepted, taking into consideration the result of the full wave calculation.

In Part II, the morphological characteristics of auroral hiss are discussed

in comparison with those of low-latitude hiss using the VLF data observed at Syowa Station and at Moshiri in Japan. Auroral hiss, considered to be a manifestation of polar substorms, is a local phenomenon and its frequency extends from a few kHz to more than 100 kHz. Low-latitude hiss, however, is closely correlated with worldwide geomagnetic storms and it is a narrow band VLF phenomenon. Together with other differences between them, it is concluded that auroral hiss is completely different from low-latitude hiss.

Although the morphological features of auroral hiss have been well known, a complete understanding of its generation mechanism has not yet been obtained. There are unsolved problems such as about two orders shortening of the calculated intensity below the observations and the existence of the threshold low-energy electron flux below which VLF hiss is not observed. These facts may suggest that a coherent plasma instability mechanism is partially involved in the generation of auroral hiss. Therefore, the investigation of the coherency of auroral hiss being planned by us may give a better understanding of the generation processes of auroral hiss.

PART I. POLARIZATION, INCIDENT AND AZIMUTHAL ANGLES OF AURORAL HISS

1. Introduction

VLF emissions known as 'hiss' are the least investigated phenomena of various kinds of emissions, because it is difficult to distinguish hiss from other noises owing to the white noise character of hiss. However, ELLIS (1959) has devised the minimum level reading circuit for the efficient detection of VLF hiss. Since then, the characteristics of the occurrence of ground-based VLF hiss have been made clear in the case of auroral hiss (MARTIN *et al.*, 1960 ; HELMS and TURTLE, 1964 ; HARANG and LARSEN, 1965 ; MOROZUMI and HELLIWELL, 1966 ; HARANG, 1968 ; NISHINO and TANAKA, 1969a ; TANAKA *et al.*, 1970 ; TANAKA, 1972) as well as in the case of low-latitude hiss (IWAI *et al.*, 1964 ; HARANG and LARSEN, 1965 ; HARANG, 1968 ; IWAI and TANAKA, 1968 ; TANAKA and KASHIWAGI, 1968 ; TANAKA *et al.*, 1974 ; HAYAKAWA *et al.*, 1975). In addition to ground-based observations, satellite experiments have provided us with abundant information (GURNETT, 1966 ; MCEWEN and BARRINGTON, 1967 ; BULLOUGH *et al.*, 1969a ; BURTIS, 1969 ; HUGHES and KAISER, 1971 ; KAISER, 1972 ; GURNETT and FRANK, 1972 ; LIM and LAASPERE, 1972 ; LAASPERE and JOHNSON, 1973 ; TAYLOR and SHAWHAN, 1974). So, the information about the occurrence of magnetospheric hiss has greatly increased during this decade.

However, very few reports have been published up to date on the measurement of the polarization, incident angle and arriving direction of VLF hiss. This seems to be due to the lack of techniques adequate for the direction finding of noise-like signals such as hiss. A DF system is important to find the exit point of the hiss, from which we can estimate the generation region of the hiss and its generation and propagation processes.

ELLIS (1960) has made directional and spaced observations of VLF hiss

with goniometer arrangements in Australia and has shown that most of VLF noise bursts probably come from the southern auroral zone.

HARANG and HAUGE (1965) have studied the arriving direction of VLF hiss by alternately switching crossed loop antennas to a pre-amplifier and investigated the polarization by displaying the pattern on a cathode ray tube, near the northern auroral zone. Their results have shown that there exist no differences between the outputs from both frames and that the ordinary VLF bursts show irregular oscillographic patterns. Then it was suggested that VLF emissions came from all directions to an observing point located within a source of bursts.

IWAI and TANAKA (1968) have measured the direction and polarization of low-latitude hiss at Moshiri (geomag. lat. 34°) in Japan and found that the observed polarization was usually linear and so the direction finding with a goniometer arrangement was effective in some cases of intense hiss. Their results have shown that the hiss observed at Moshiri has propagated from the north.

VERSHININ (1970) has studied the arriving direction of hiss by changing the direction of magnetic antenna orientation and found that at the appearance of isolated bursts of VLF hiss, the signal level is independent of the direction of the antenna axis when the source bursts are located over the observing point.

Taking the above results by a few workers into account, we come to the conclusion that the DF experiment using the goniometer arrangement or the switching method are not effective for auroral hiss downcoming over the observing point. For this reason, we have used a DF method based on the analysis of Lissajous' figures of electric and magnetic fields displayed on cathode ray tubes and then we were able to get information on the incident angle and arriving direction. Also the polarization has been continuously measured by means of a polarimeter.

In this part, we discuss the system of equipment used for measuring the polarization, incident angle and arriving direction of auroral hiss and we show the obtained results. Then a considerable discussion of the utility of our DF method is given. Finally, we propose a new DF system devised for noise-like signals such as auroral hiss, which is considered to be more effective for noise-like waves than the method based on Lissajous' figures. It is hoped that this system will be in operation during the forthcoming International Magnetospheric Study.

2. Instrumentation

The program of our auroral hiss observations carried out at Syowa Station (geomag. lat. −69.6°) during the period of 1967 to 1970, consisted of three items, *i. e.*,

1. observation of auroral hiss intensity
2. continuous recording of right- and left-handed polarized components
3. measurements of polarization, incident angle and arriving direction based on Lissajous' figures displayed on a cathode ray tube (hereafter this method is called as CRT method).

2.1. Principle of the observation

Methods for observing physical characteristics such as polarization, incident

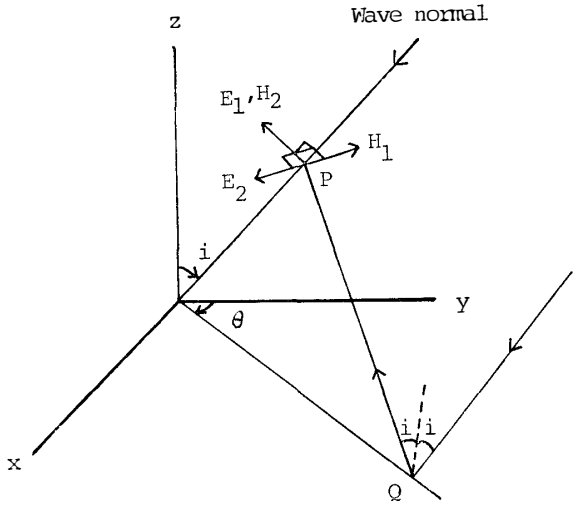

Fig. 1. Configuration of the problem. The electromagnetic fields at P are composed of those of a direct ray and those of a ground-reflected ray. The downgoing wave is assumed to have an incident angle of i and azimuthal direction of 0. E_1 and H_1 correspond to TM mode, while E_2 and H_2 TE mode.

angle and arriving direction of radio waves have been discussed by several workers (CARTWRIGHT, 1961 ; IWAI, 1962 ; DELLOUE and GARNIER, 1963 ; IWAI and TANAKA, 1968 ; NISHINO and TANAKA, 1969b ; MOISER and GURNETT, 1969 ; TANAKA, 1972 ; COUSINS, 1972 ; BULLOUGH and SAGREDO, 1973 ; TSURUDA and HAYASHI, 1975). We first show the principle of our method of measuring wave characteristics. The configuration of the problem is shown in Fig. 1 and the electromagnetic fields at a point of P are given by :

$$H_x = \left\{-1+\rho_2 \exp\left(-j\frac{4\pi h}{\lambda}\cos i\right)\right\} H_2 \cos i \cdot \sin\theta$$
$$-\left\{1+\rho_1 \exp\left(-j\frac{4\pi h}{\lambda}\cos i\right)\right\} H_1 \cos\theta$$

$$H_y = \left\{-1+\rho_2 \exp\left(-j\frac{4\pi h}{\lambda}\cos i\right)\right\} H_2 \cos i \cdot \cos\theta$$
$$+\left\{1+\rho_1 \exp\left(-j\frac{4\pi h}{\lambda}\cos i\right)\right\} H_1 \sin\theta$$

$$H_z = \left\{1+\rho_2 \exp\left(-j\frac{4\pi h}{\lambda}\cos i\right)\right\} H_2 \sin i$$

$$E_x = \left\{-1+\rho_1 \exp\left\{-j\frac{4\pi h}{\lambda}\cos i\right)\right\} E_1 \cos i \cdot \sin\theta$$
$$+\left\{1+\rho_2 \exp\left(-j\frac{4\pi h}{\lambda}\cos i\right)\right\} E_2 \cos\theta$$

$$E_y = \left\{-1+\rho_1 \exp\left(-j\frac{4\pi h}{\lambda}\cos i\right)\right\} E_1 \cos i \cdot \cos\theta$$
$$-\left\{1+\rho_2 \exp\left(-j\frac{4\pi h}{\lambda}\cos i\right)\right\} E_2 \sin\theta$$

$$E_z = \left\{1+\rho_1 \exp\left(-j\frac{4\pi h}{\lambda}\cos i\right)\right\} E_1 \sin \imath$$

where

x, y, z : Cartesian coordinates
z is directed vertically upward.
y is directed toward geographical north and the $x-y$ plane is the ground.

ω : angular wave frequency. A time factor exp ($j\omega t$) is used in this paper.

i : incident angle

θ : azimuthal angle

H_x, H_y, H_z : x, y and z components of magnetic fields at the point P

E_1, H_1 : electric and magnetic fields of TM mode wave
E_2, H_2 : electric and magnetic fields of TE mode wave
ρ_1, ρ_2 : complex ground reflection coefficients of TM and TE mode waves
λ : wavelength
h : height of the receiving point P

Here the definition of the TM mode is that the wave electric field lies in the incident plane, whereas in the TE mode the electric field is directed perpendicular to the incident plane. Then we make the following three assumptions.

(a) The auroral hiss is generally a downcoming plane wave and is elliptically polarized.

(b) The ground is flat and perfectly conductive.

(c) The wave is a monochromatic sine wave.

Assumption (a) is probably reasonable in the case of the reception of auroral hiss within the auroral region such as Syowa Station.

Next, it is acceptable, in most cases except in the case of nearly horizontal direction of arrival, to assume that the ground is perfectly conductive at VLF and even at LF. Finally, assumption (c) can be justified when narrow band pass filters are used and we discuss the patterns during the initial and a few more cycles. Based on the above assumptions, we then get the following relationships. $\rho_1=1$, $\rho_2=-1$ and $\lambda \gg h$
and hence

$$H_x=-2A_2\cos i\cdot\sin\theta\cdot\sin(\omega t+\phi)-2A_1\cos\theta\cdot\sin\omega t$$
$$H_y=-2A_2\cos i\cdot\cos\theta\cdot\sin(\omega t+\phi)+2A_1\sin\theta\cdot\sin\omega t$$
$$E_z=2A_1\sin i\cdot\sin\omega t$$
$$H_z=E_x=E_y=0$$

where, $H_1=A_1\sin\omega t$
$H_2=A_2\sin(\omega t+\phi)$
$E_1=A_1\sin\omega t$

A_1 and A_2 are the amplitudes of the magnetic fields of TM and TE mode waves, respectively, and ϕ is the phase difference between the TM and TE mode waves. Hence, it is found that only three electromagnetic field components of H_x, H_y and E_z have to be discussed at VLF range. These three field components are used to deduce the incident angle, azimuthal direction and also polarization.

2.1.1. Observation of polarization with polarimeter and pen-oscillograph method

The use of the expressions of three components discussed above makes it

possible to deduce the polarization as in the following way. The H_x component is led and lagged in phase by right angle by passing it through a phase shifter and then the components led and lagged by 90° are added to H_y, respectively. Accordingly we get the following relationships.

$$\text{Amplitude of } (H_x^{\pm}+H_y)=2\{(A_2^2\cos^2 i+A_1^2)\pm 2A_2A_1\cos i\cdot\sin\phi\}^{1/2}$$

We now define the C value in the following way.

$$C=\frac{\text{amplitude of } (H_x^-+H_y)}{\text{amplitude of } (H_x^++H_y)}=\left(\frac{k^2+1-2k\sin\phi}{k^2+1+2k\sin\phi}\right)^{1/2}=R/L$$

where, H_x^+ : H_x component led in phase by 90°
H_x^- : H_x component lagged in phase by 90°
$k=A_2\cos i/A_1$
R/L : the ratio of R- to L-components

Then,
if $C>1$: right-handed elliptically polarized
if $C<1$: left-handed elliptically polarized
if $C=1$: linearly polarized

The right-handed sense means that the electric and magnetic vectors rotate clockwise when the observer is looking in the direction of the earth's magnetic field. How the C values vary with the values of ϕ are shown in Fig. 2 with a parameter of k.

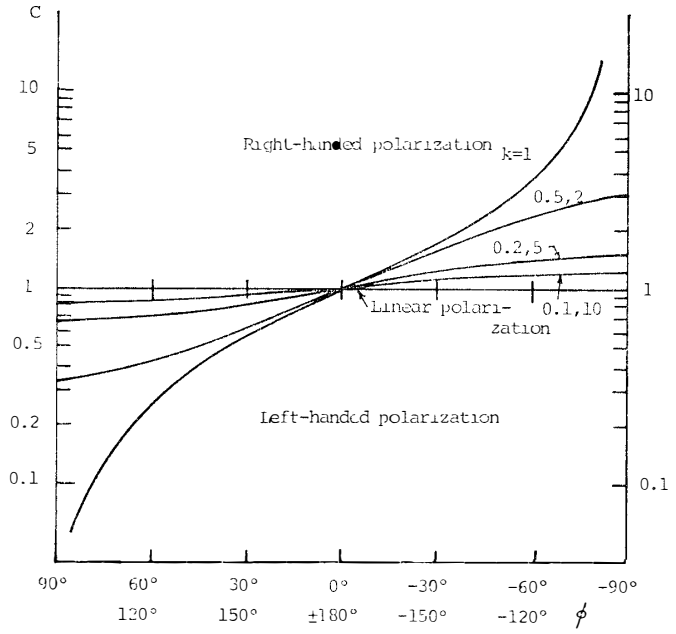

Fig. 2. Variation of C value with φ with a parameter of k. C>1 indicates the right-handed polarization, whereas C<1 the left-handed polarization.

2.1.2. *Observation with CRT method*

In order to obtain the equivalent rotation of loop antennas, the goniometer is inserted in the receiving systems. When the rotation angle of a goniometer is equal to the azimuthal angle of the received signal, the Lissajous' figure of H_x and E_z becomes linear and then the azimuthal as well as the incident angles can be immediately obtained (IWAI and TANAKA, 1968). However, the DF system making use of the goniometer was found to be generally non-effective at Syowa Station. The reason may be attributed to the noise-like nature of auroral hiss which consists, in most cases, of wave components downcoming over the observing point from multiple directions in azimuth and incidence. Hence, we explain in this section an observing method with fixed crossed loops. So, the H_x-H_y figure displayed only during the plus half cycles of E_z (Fig. 3-1), and the H_x-E_z figure (Fig. 3-2) are used to find the wave characteristics. When $E_z=0$, $H_x/H_y=\tan\theta$ for the line cutting the half of the ellipse. Thus, the symmetric line of the cutting line with respect to the straight line $H_x=H_y$ gives the arriving direction. And the arriving direction is determined without the ambiguity of 180° by a simple analysis. If the coordinate axes are rotated counter-clockwise by an angle θ and the new axes are written as $\bar{H}_x$ and $\bar{H}_y$, then $\bar{H}_x$ and $\bar{H}_y$ can be given by

$$\bar{H}_x=-2A_1\sin\omega t,\ \bar{H}_y=-2A_2\sin(\omega t+\phi)\cos i$$

This is the same expression as H_x and H_y with $\theta=0°$. Then we can obtain the values of $A_2\cos i/A_1(=k)$ and $|\sin\phi|$, as shown in Fig. 4 and ϕ can be estimated by a simple manipulation. The H_x-E_z figure is, in general, an ellipse and we get the relationship $m/p=\sin i/(k|\sin\theta\cdot\sin\phi|)$, from which we can determine the value of i. Thus, all physical quantities can be obtained

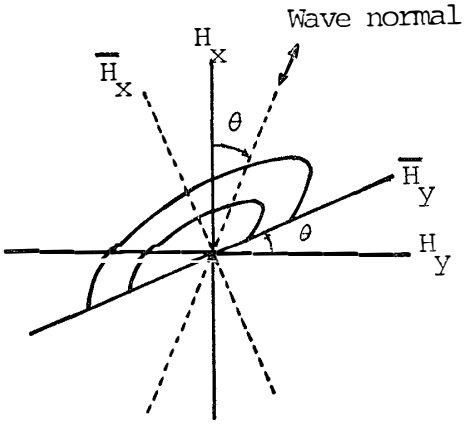

Fig. 3-1. H_x-H_y figure during plus half cycle of E_z and new coordinate axes of $\bar{H}_x$ and $\bar{H}_y$.

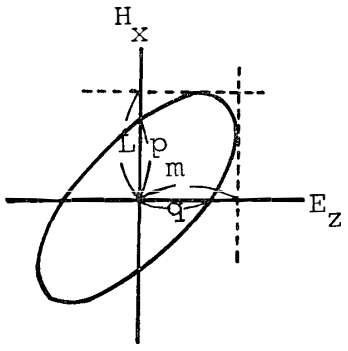

Fig. 3-2. E_x-E_z pattern. The values of m and p satisfy the relationship of $m/p=\sin i/(k|\sin\theta\cdot\sin\phi|)$.

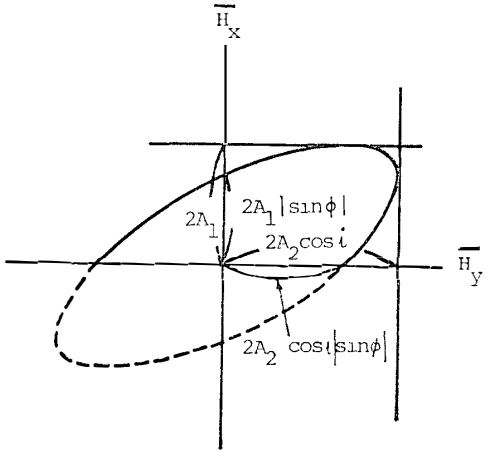

Fig. 4. $\bar{H}_x$-$\bar{H}_y$ pattern to deduce $A_2 \cos i/A_1(=k)$ and $|\sin\phi|$.

without any ambiguity.

The aforementioned treatment is valid for a single wave. The above discussion is, however, reasonably justified only when the intensity of one wave is much more dominant that of other waves, even if several signals are simultaneously received from multiple directions within a source area.

2.2. Observing technique

The block diagram of the instrument is shown in Fig. 5. The antenna system consists of a pair of crossed loops with their planes oriented in geographical N-S and E-W directions and a vertical antenna. Each loop antenna is of triangle type of two turns and its dimension is 20 m in height and 40 m at the base. The vertical antenna is a pipe of 10 m long. In order to reduce the interferring disturbances induced by the very low conductivity of the ground, the counterpoise is set radially around the vertical antenna with 35 copper wires of 15 m long. As a result, the value of S/N is improved by more than 10 dB. The pre-amplifiers are installed just under the antennas and each of the output signals is carried by a twin-axial cable of 300–350 m long to the main amplifier in the observation room. The signals passed through the main amplifiers are supplied to the intensity meter, polarimeter and cathode ray tubes.

The intensity meter consists of narrow band amplifiers and pen-oscillographs. By narrow band amplifiers with band pass filters of $Q=10$, the signals (we generally use the N-S signal) are amplified at eight frequencies centered at 0.75, 2, 5, 8, 12, 25, 40 and 70 kHz and the signal at each frequency is rectified to d-c and averaged for 10 milliseconds and then fed to the resistance-

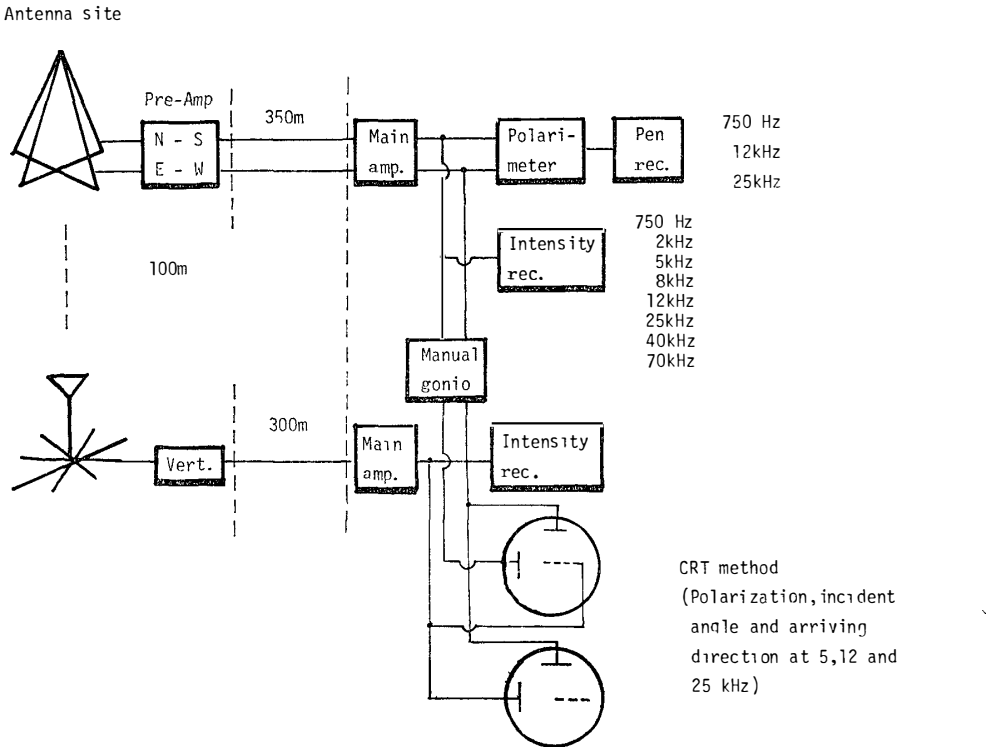

Fig. 5. Block diagram of the apparatus installed at Syowa Station. The electromagnetic signals passed through the main amplifiers are supplied to the intensity meter, polarimeter and cathode ray tubes for measuring the incident and azimuthal directions.

capacitance circuit with a charging time constant of 5 seconds and a discharging time constant of 2 milliseconds. Its d-c output is recorded on a chart paper moving at 10 cm/hour. In the receiving frequency range of VLF to LF the average intensity of auroral hiss is about 20 dB above the threshold level determined by undesirable signals such as atmospherics and power line noises. And the threshold level is also more than 10 dB above the set noise level of $\sim 2 \times 10^{-18}$ Wm^{-2} Hz^{-1}.

2.2.1. Observation of polarization with polarimeter and pen-oscillograph method

Fig. 6 shows the block diagram of the polarimeter and pen-oscillograph system. The polarimeter is composed of a pair of phase shifters and two band-pass amplifiers. With a pair of phase shifters, the N–S signal is led in phase by a right angle at the specific frequencies and added to the E–W signal. Similarly, the N–S signal lagged by 90° is added to the E–W signal. Then, we can decompose the signals into right- and left-handed polarized components. The decomposed signals are introduced to the band pass amplifiers with band pass filters whose center frequencies are 0.75, 12 and 25 kHz and whose Q value is 40. Then each signal is supplied to a detecting circuit with the

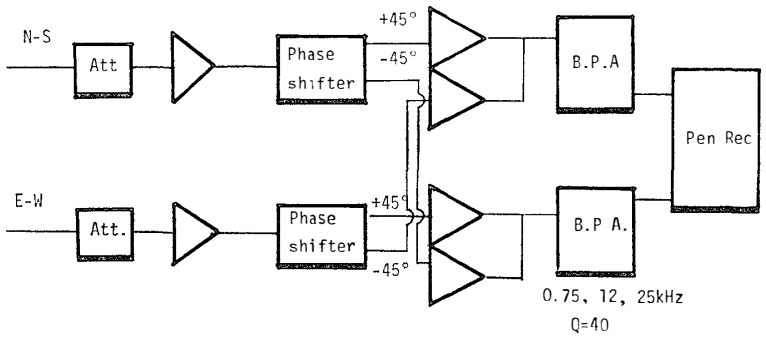

Fig. 6. Block diagram of the polarimeter and pen-oscillograph system. The polarimeter consists of a pair of phase shifters and two band-pass amplifiers.

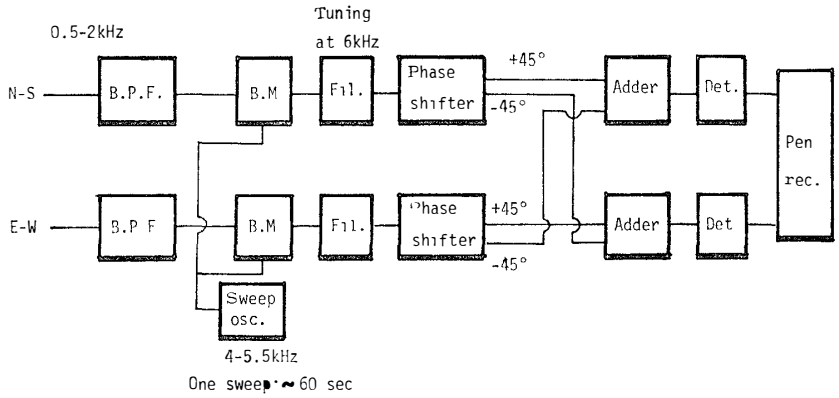

Fig. 7. Block diagram of the frequency-swept polarimeter to measure the polarization of ELF hiss in the frequency range of 0.5-2kHz. One sweep is taken to be about 60 sec.

same properties as the intensity meter and the output is recorded on a chart paper moving at 10 cm/hour.

In 1970 we began the measurement of polarization at a frequency of 50 kHz to investgate the polarization characteristics at higher frequencies. Moreover, a frequency-swept polarimeter (0.5–2 kHz) was in operation, which was able to measure the frequency dependence of the polarization, especially, at lower frequency ranges in which there is an interesting phenomenon of ELF hiss appearing predominantly at daytime in summer. Its block diagram is illustrated in Fig, 7.

2.2.2. Observation of polarization, incident angle and arriving direction with CRT method

Fig. 8 shows the block diagram of the CRT method for the measurement of polarization, incident angle and arriving direction at three specific frequencies

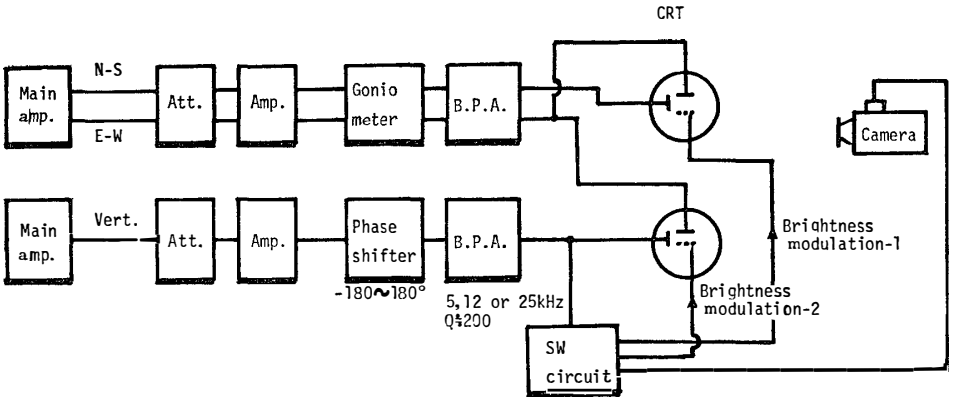

Fig. 8. Block diagram of CRT method measuring the polarization, incident angle and arriving direction at 5, 12 and 25 kHz.

of 5, 12 and 25 kHz. The signals of NS and EW channels of the loop antenna system are given to a goniometer and then supplied to the band pass amplifiers in which the phase and gain are accurately adjusted so as to eliminate the differences of phase and gain induced in the two receiving systems. When the signal received by the vertical antenna is given to a CRT, the phase shift caused in the whole receiving system involving the antenna, must be equalized to that of NS and EW signals. So, the phase of the vertical signal is adjusted by using the phase shifter. These phase adjustments of the receiving systems are made by giving test signals to the dummy antenna circuit installed instead of the observing antennas. The outputs from NS and EW channel band pass amplifiers ($Q=200$) are introduced to a CRT. An output from the vertical channel band pass amplifier ($Q=200$) and either NS or EW output are given to the other CRT. The output from the vertical channel is also supplied to the switching circuit, by means of which the two output signals modulate the brightness of the pictures on the two cathode ray tubes, respectively.

Fig. 9 shows the block diagram of the switching circuit. When a signal to start photographing is given, the interval (1, 2, 5 or 10 seconds) and frame number (1, 2, 4 or 8) of the photographing are selected in the interval and frame number control circuit. On the other hand, the starting signal triggers the shutter of the camera. A gate signal which synchronizes with the shutters's movement is shaped and then supplied to a one-shot multivibrator in which the duration of brightness modulation is arbitrarily chosen. The output from the one-shot multivibrator is modified in the integral circuit so that a Lissajous' figure fades gradually into a tail-like shape. As the result, we can easily know the sense of rotation of the magnetic field. We want the CRT display of the pictures described by the N-S and E-W signals only when the amplitude of the vertical signal is greater than or equal to zero level. So d-c bias is added so that the Schmitt triggering starts at the zero

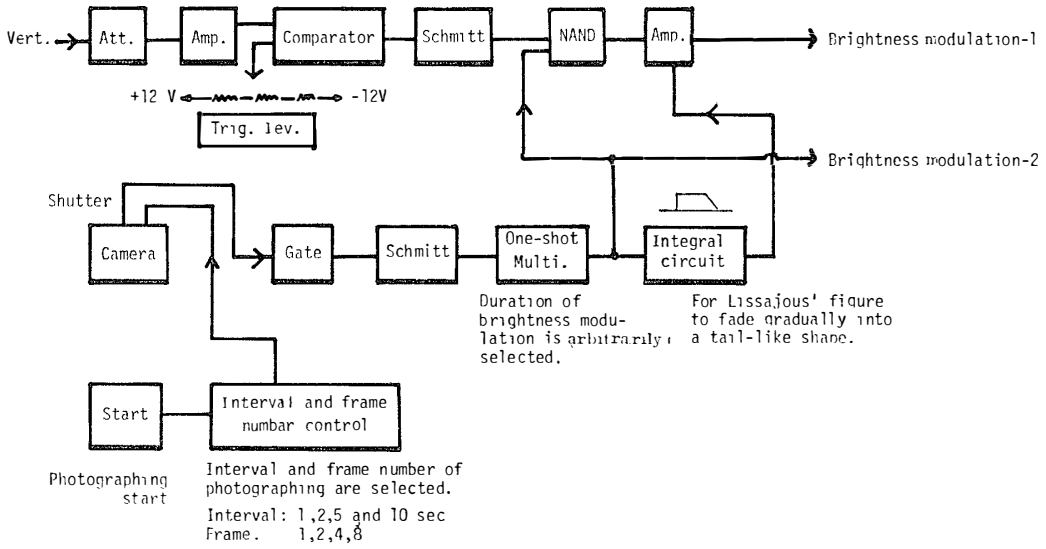

Fig. 9. Block diagram of the switching circuit.

level of the vertical signal. Then the output from the Schmitt circuit is modified by the outputs from the one-shot multivibrator and integral circuit. The modified signal is added to the cathode of the CRT so that the brightness modulation is begun at the zero level of the vertical signal and continues only during plus half cycles.

At the station where the sources of auroral hiss are just overhead of the observing point and where a few waves with not so large incident angles are received at the same time, it is generally difficult to use a goniometer arrangement. For our practical observation, a goniometer arrangement was not effective, and so we kept the goniometer fixed. The figure described by the N-S and E-W signals is, in practice, displayed only during a few plus half cycles of the vertical signal. The two CRT patterns are simultaneously photographed and all physical properties of auroral hiss are analysed from the photograph.

3. Observed Results

3.1. General features of auroral hiss

We briefly show some data obtained with the intensity meter and polarimeter. Fig. 10 shows the diurnal and seasonal variations of the occurrence frequency of the auroral hiss at 12 kHz. The corresponding diurnal and seasonal variations in the frequency range of 5 to 25 kHz show the similar trend, though there exists a difference of the occurrence number with frequency (TANAKA, 1972). The auroral hiss is most active before the magnetic midnight and its occurrence is concentrated in the local nighttime. The hiss appears predominantly in winter and at equinoxes and then it occurs very infrequently in summer. The decrease of its occurrence rate in summer can be attributed to the ionospheric absorption (HARANG and HAUGE, 1965).

The VLF hiss observed at Syowa Station may be divided into the steady and impulsive types. Figs. 11–18 illustrate several typical data, in which are given the temporal variations of the auroral hiss events, their polarizations, geomagnetic H-components and cosmic noise absorptions (CNA) at 30 MHz.

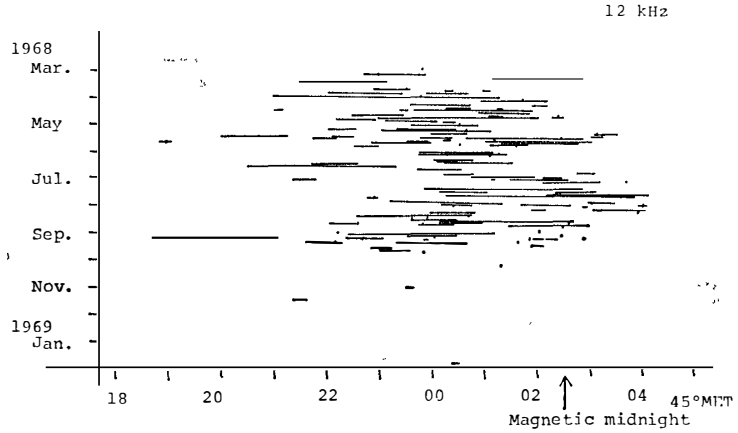

Fig. 10. Diurnal and seasonal variations of the occurrence rate of VLF hiss. Each dot represents the peak of the event. The hiss appears predominantly before magnetic midnight.

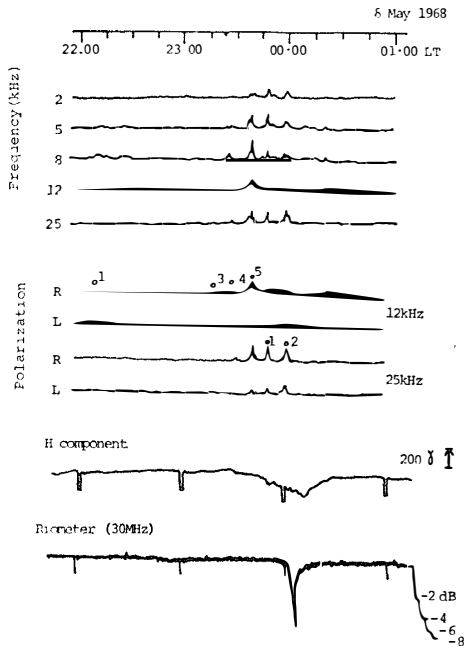

Fig. 11. An example of the temporal variation of intensity and polarization of the hiss event on 8 May 1968. The corresponding variations of geomagnetic H component and riometer absorption are also illustrated.

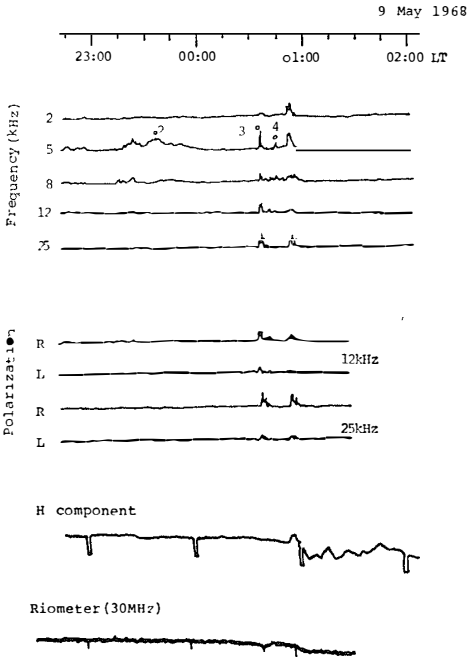

Fig. 12. The hiss event on 9 May 1968.

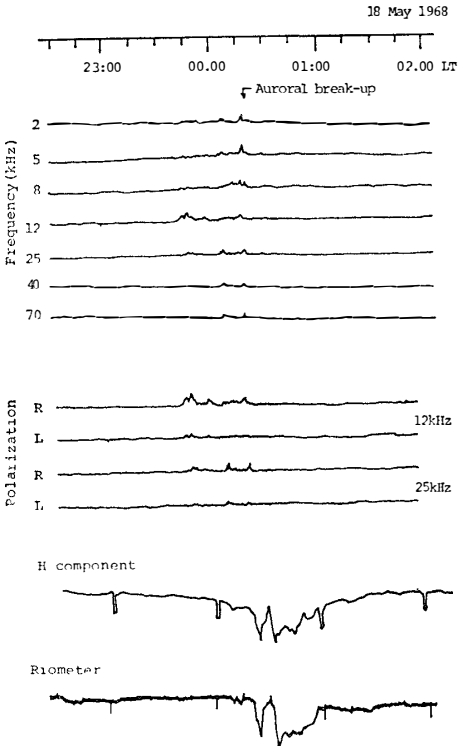

Fig. 13. The hiss event on 18 May 1968.

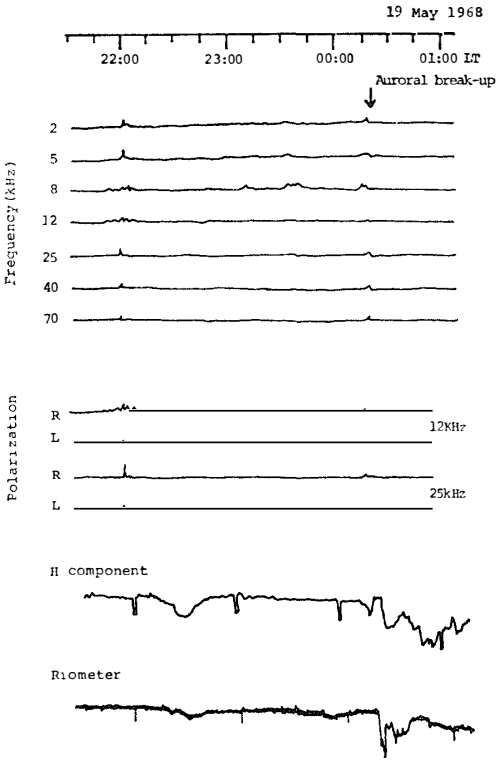

Fig. 14. The hiss event on 19 May 1968.

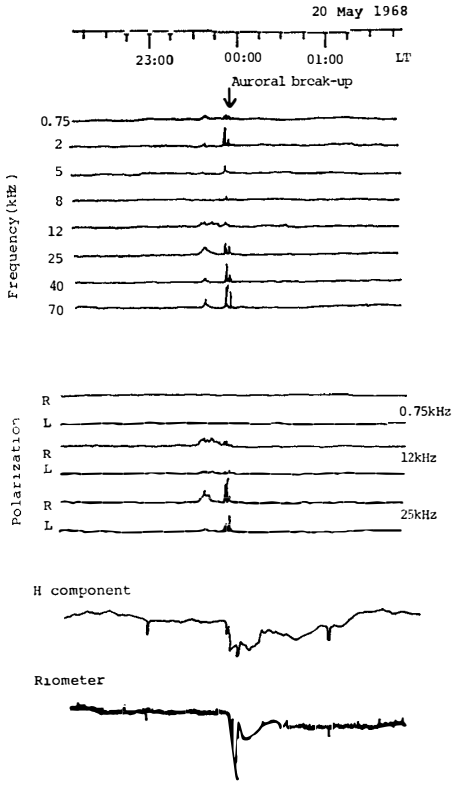

Fig. 15. The hiss event on 20 May 1968.

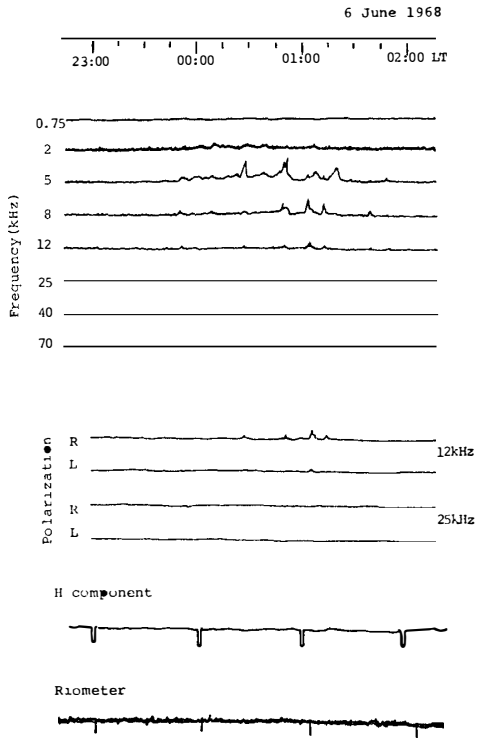

Fig. 16. The hiss event on 6 June 1968.

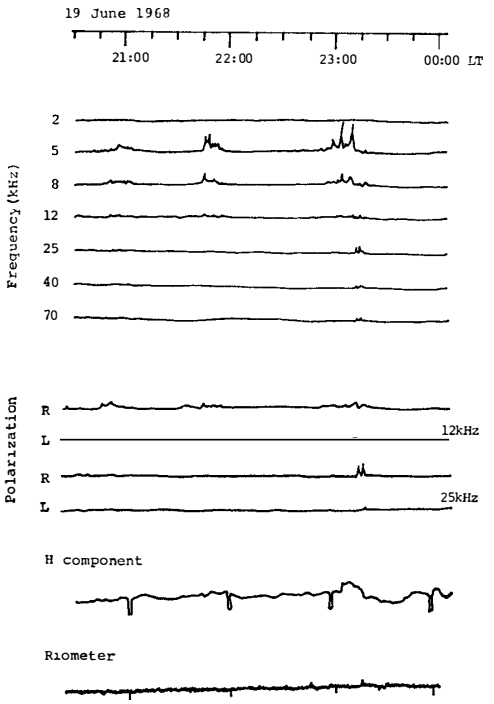

Fig. 17. The hiss event on 19 June 1968.

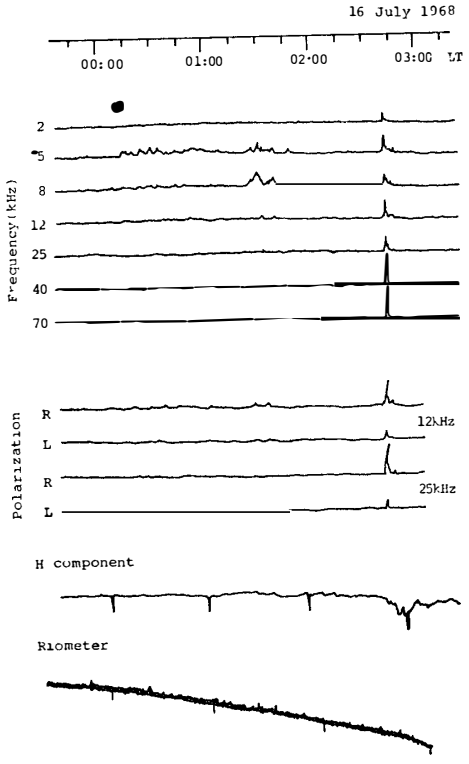

Fig. 18. The hiss event on 16 July 1968.

The steady type auroral hiss which appears in association with moderate geomagnetic activity and weak CNA, continues from ten to several tens of minutes and dominates in the lower frequency range of 5–12 kHz and usually occurs on the evening side of the nighttime, as shown in Figs. 12, 16, 17 and 18. Near magnetic midnight an aurora breaks up around the zenith and the auroral break-up is always followed by sharp and large fluctuations of the magnetic H-component and CNA. There appears to be usually a time delay of a few minutes between the outburst of aurora and the increase in CNA (HOLT and OMHOLT, 1962). An impulsive type auroral hiss occurs almost simultaneously with the auroral break-up and falls sharply within a short period (about several minutes) before the maximum activity of the aurora and its frequency spectrum widens, as shown in Figs. 13, 14 and 15. Even when an auroral break-up does not occur or cannot be observed, an impulsive auroral hiss with a wide band frequency range sometimes appears, which is not always followed by a large geomagnetic fluctuation and is less associated with CNA, as shown in Figs. 11, 12, 14, 17 and 18.

The following recent results should be taken into account in order to get a better understanding of our aforementioned general features of auroral hiss. Using the correlated study between ground-based auroral emissions and VLF emissions by the Injun 5 satellite, MOSIER and GURNETT (1972) have found that not all auroral-light emissions are associated with VLF emissions. This finding is consistent with the earlier result of GURNETT (1966), who has indicated that VLF hiss and auroral-light emissions are produced by electrons of somewhat different energies. Recently GURNETT and FRANK (1972) have provided direct verification of the association between the auroral hiss and intense fluxes of electrons of the order of 100 eV. The auroral-light emissions, however, are generally generated by electrons with somewhat higher energy of the order of 1 to 10 keV. If the precipitated electron energy spectrum is sufficiently broad, both auroral hiss and auroral-light emissions are observed (MOSIER and GURNETT, 1972). On the other hand, the auroral electron precipitation events at 10 keV during the entire life of OV3–1 satellite are found to have a good correlation to k_p-indices (KUCK, 1970), but no significant correlation was found between k_p and auroral hiss based on the Injun 3 satellite data (GURNETT, 1966). Considering the above facts, the relationship of the association between VLF hiss and other geophysical phenomena seems likely to depend on the energy spectrum of the precipitating electrons.

The intensity of auroral hiss is positively correlated to weak CNA's, as is shown in Fig. 19. This result coincides with the earlier result obtained by HARANG and LARSEN (1965) based on data at Tromsø (67° geomag. lat.). The geomagnetic perturbations and CNA's take place, apparently, in phase,

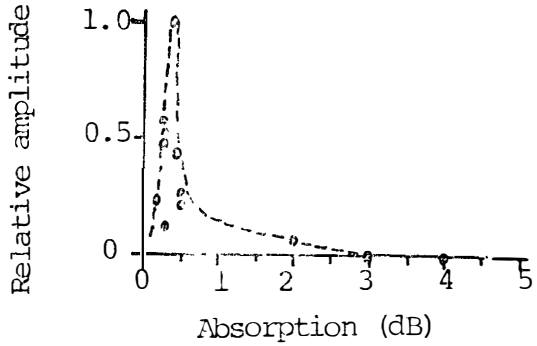

Fig. 19. Relationship between the hiss intensity at 12kHz and the riometer dip. VLF hiss appears during small absorption dips in the riometer.

because both phenomena are caused by the auroral particles precipitating into the ionosphere. But, Figs. 17 and 18 show that the CNA has a lower correlation to aurroal hiss than does geomagnetic variation. This may be partially due to the fact that the CNA is mainly attributed to the enhanced ionization of the lower ionosphere produced by electrons with somewhat higher energies. Other causes lie in the method of riometer observation. The cosmic noise intensity at Syowa Station was recorded by a standard riometer connected to a vertically directed five-element Yagi antenna, so that the riometer is able to record cosmic noise intensity which is only sharply directed toward the vertical direction. Also, it is not always easy to distinguish, in practice, a small dip in the riometer datum, because of the relatively low S/N ratio.

3.2. Measurement of polarization, incident angle and arriving direction with CRT method

We could, unfortunately, obtain little desirable data by the CRT method. This lack of available data seems to be caused by technical problems, atmospherics and others. The most serious problem in the observational technique was unwanted signals such as power line noises and atmospherics which are to be excluded. The vertical antenna installed on the ground of low conductivity easily picks up the power noises, and so the counterpoise was set to improve this demerit. However, in spite of our efforts, complete improvement was not achieved. Then the essential trouble was the influence of atmospherics. Atmospherics are known to come from almost horizontal direction and their intensity is higher than the hiss even in winter and equinoxes. The intensity level of atmospherics received by the vertical antenna was, in most cases, above the level of the auroral hiss coming down with a small incident angle. In the

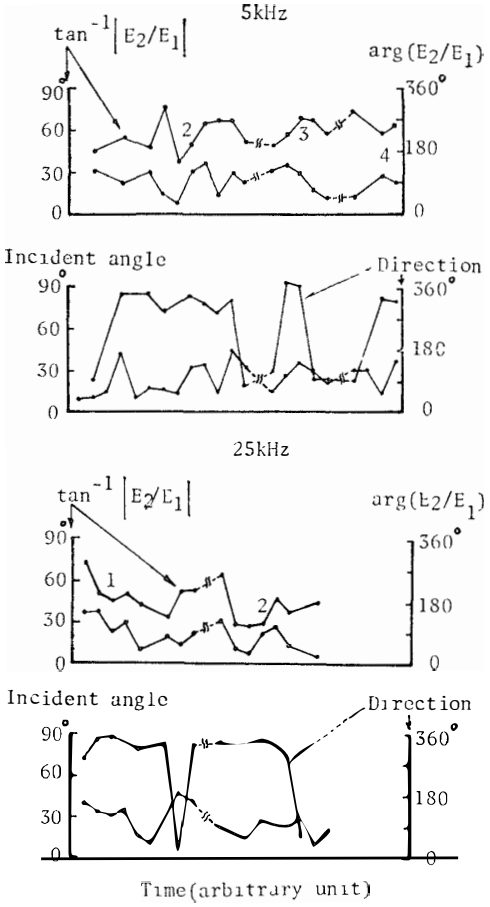

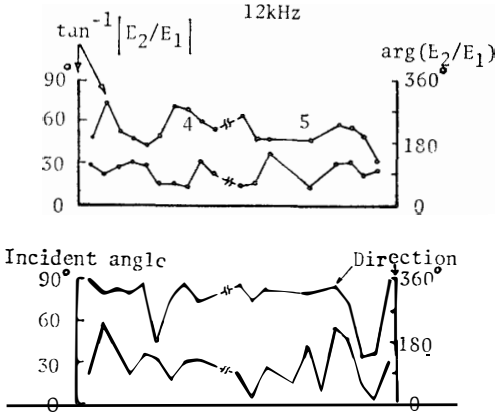

Fig. 20. Examples of the temporal variation of the polarization, incident angle and arriving direction during the hiss event. E_2/E_1 indicates the ratio of perpendicular to parallel polarization in the electric vector. The data on 5kHz correspond to the event in Fig. 12 and the numbers in the figure correspond to the same numbers during the event in Fig. 12. The abscissa indicating the time is given in arbitrary unit. The results at 12 and 25 kHz correspond to the hiss event in Fig. 11. The arriving direction is measured clockwise from the geomagnetic north.

automatic observation, the brightness modulation was often operated by the triggering signal caused by atmospherics. In the case of manually controlled observation the observational timing was very difficult, because it was a happening to catch the initial and a few more cycles of isolated and sharp auroral hiss. Therefore, the resultant patterns on the CRT were disturbed by undesirable signals in most cases or noise type patterns were observed which were probably due to multiple waves received simultaneously. Fig. 20 shows some examples of the data of wave characteristics obtained with the CRT method for the VLF events shown in Figs. 11 and 12. The number beside the curve in the figure corresponds to the same number of VLF hiss event in Figs. 11 and 12. It is found from this figure that the auroral hiss comes down with not so a large incident angle and nearly along the magnetic meridian plane. Fig. 21 shows a few of the oscillographic patterns from which these physical quantities are deduced.

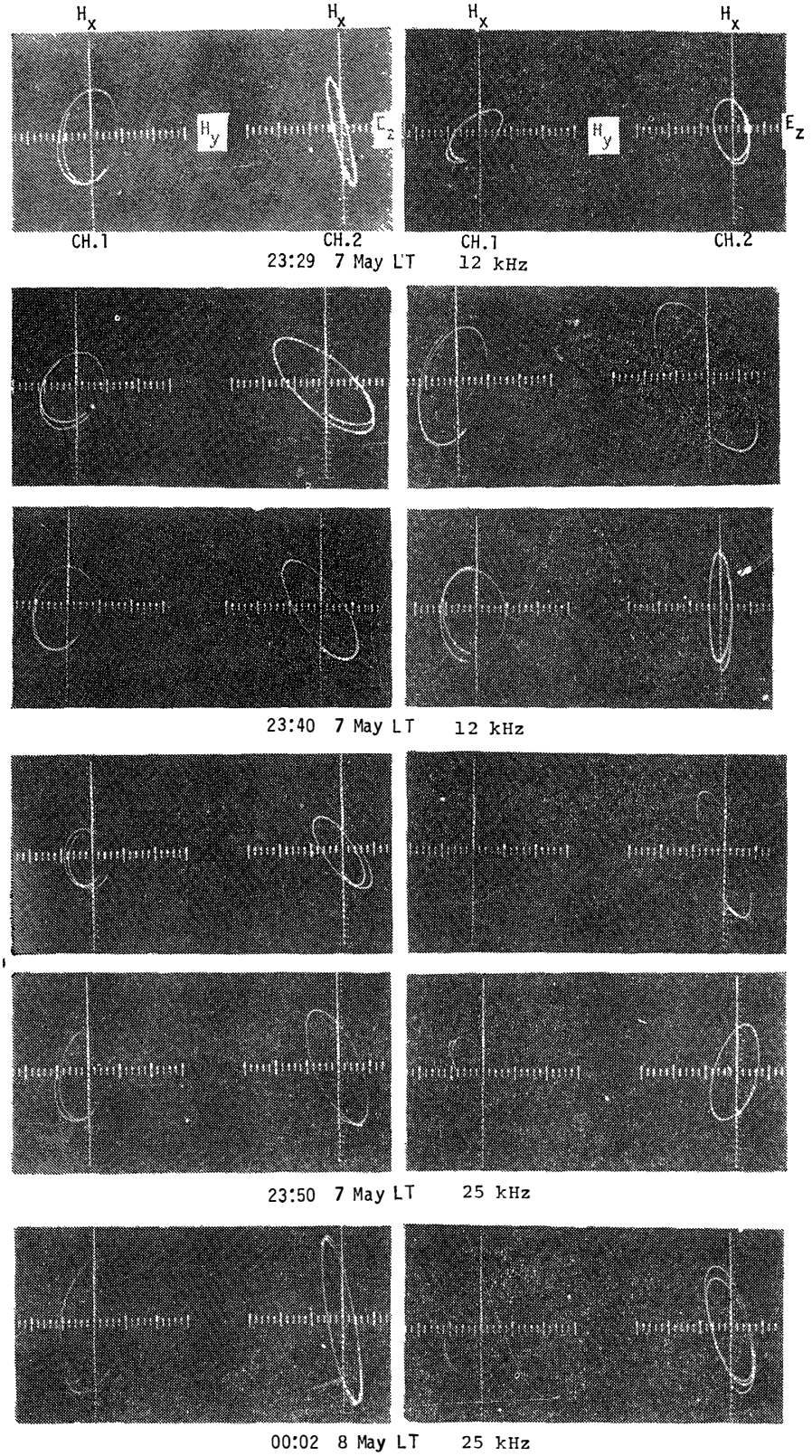

Fig. 21. Examples of oscillographic patterns. H_x and H_y are the geographically east and north components of magnetic field and E_z is the vertical component of electric field.

3.3. Polarizaiton with polarimeter and pen-oscillograph method

By means of the polarimeter, auroral hiss is divided into R- and L-components and then the two components are recorded on chart paper. Fig. 22 shows the seasonal variation of the R/L ratios at the peak levels of the auroral hiss at 12 kHz and 25 kHz obtained in the observation of 1968. This figure suggests that there are slight variations in R/L values with receiving frequencies. To study in further detail the suggested difference, the polarization measurement at 50 kHz was added in 1970 and a typical datum of the variation of polarization with frequency is shown in Fig. 23. The occurrence histograms of the R/L values are presented in Fig. 24. It is found from these two figures that the occurrence distribution of the R/L values are not always similar in different frequencies and such differences are likely to be significant and are closely related with the propagation conditions in the ionosphere and the exosphere.

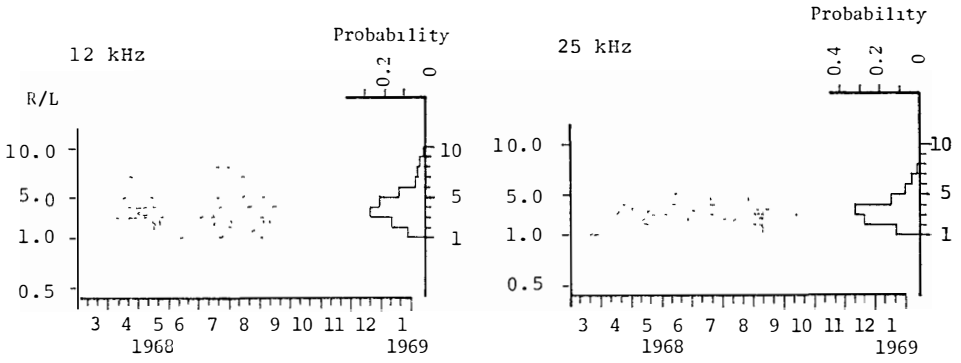

Fig. 22. Seasonal variations of R/L valus at 12 and 25 kHz and the occurrence probabilities.

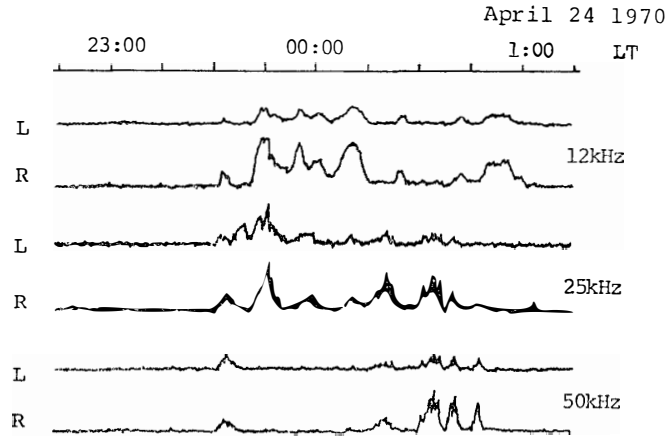

Fig. 23. An example of the temporal variation of the polarization at 12, 25 and 50 kHz of the hiss event on 24 April, 1970.

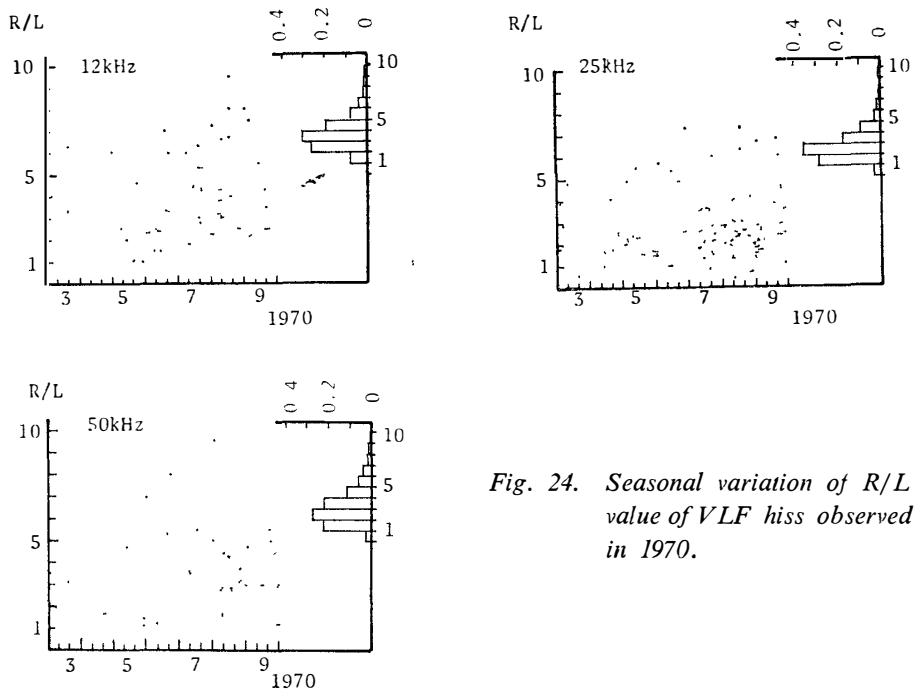

Fig. 24. Seasonal variation of R/L value of VLF hiss observed in 1970.

Similar to our results, HARANG and HAUGE (1965) have found that the auroral hiss comes approximately vertically downwards along the earth's magnetic field line in a whistler mode, although their result was not obtained by experiment alone and it involves some theoretical considerations. But the assumption that a single or multiple waves propagate downward nearly along the earth's magnetic field line intersecting Syowa Station, cannot account for our results of the scattered polarization shown in Figs. 22 and 24. This point needs further consideration and is discussed in Section 4.

As to ELF hiss occurring usually in the daytime in summer, polarization observation at a point frequency of 750 Hz was carried out during the period of 1967 to 1970. In 1970 we introduced the measurement of the polarization of ELF hiss (0.5–2 kHz) with the frequency-swept polarimeter. Examples of the temporal variation of the polarization 750 Hz are given in Fig. 25 and the seasonal variation of the R/L values of 750 Hz at hiss is illustrated in Fig. 26. Fig. 27 shows a datum of the frequency variation of the polarization obtained with the frequency-swept polarimeter. These three figures show that ELF hiss is slightly right-handed polarized.

We now investigate the dependence of the polarization ratio R/L upon the geomagnetic activity and other geophysical parameters. Fig. 28 represents the R/L value of the auroral hiss at 12 kHz versus the K-index during the time period of 21–24 LT and Fig. 29 gives the occurrence probability of R/L

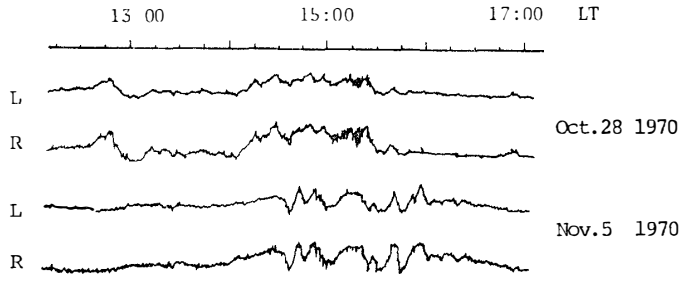

Fig. 25. Examples of the temporal variation of the polarization at 750 Hz. The upper data refer to the event on 28 October 1970, and the lower to the event on 5 November 1970.

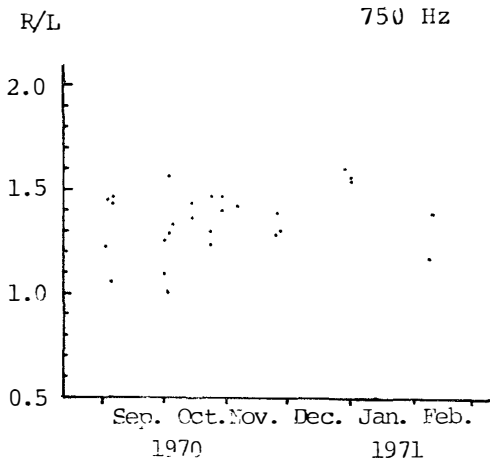

Fig. 26. Seasonal variation of R/L of ELF hiss at 750 Hz.

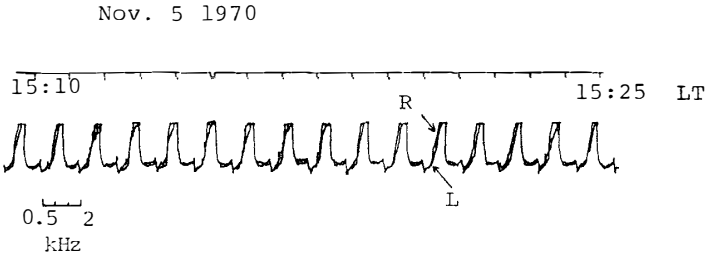

Fig. 27. An example of the polarization of ELF hiss obtained with the frequency-swept polarimeter. Curves with higher levels represent the R-component, and the curves with lower levels the L-component. The R- and L-components at a frequency during one sweep are read as the heights above the zero level, and we can know the value of R/L. The ordinate is given in linear scale.

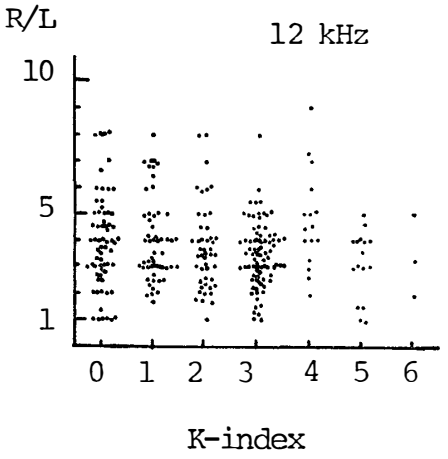

Fig. 28. Relationship between R/L at 12 kHz and K-index during the time period of 21:00 to 24:00h LT.

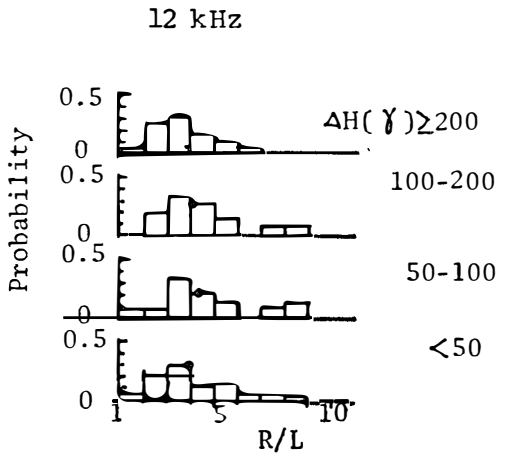

Fig. 29. Occurrence probability of R/L at 12 kHz in four ranges of geomagnetic activity. Dots indicate the average values in each range.

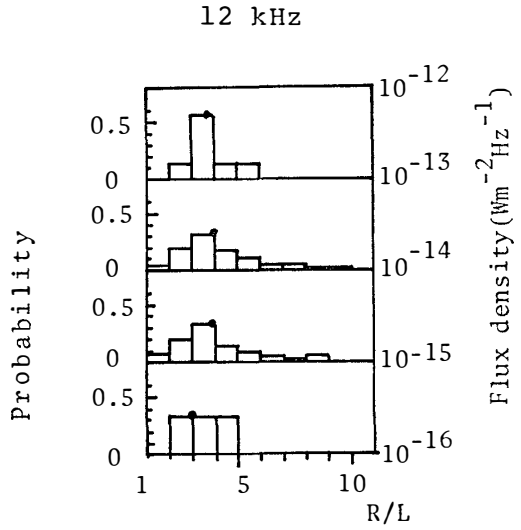

Fig. 30. Occurrence probability of R/L at 12 kHz for four ranges of flux density. Dots represent the average valus for each range.

at 12 kHz for four ranges of geomagnetic activity. It seems from these two figures that the polarization of the auroral hiss is independent of the geomagnetic activity, although its occurrence depends on the geomagnetic activity as was discussed in 3.1.

The precipitating auroral particles which have a good correlation with geomagnetic activity enhance the ionization of the atmosphere, especially, in the lower ionosphere where the QL approximaiton for VLF wave propagation is invalid and where also the wave couplings are supposed to occur. The

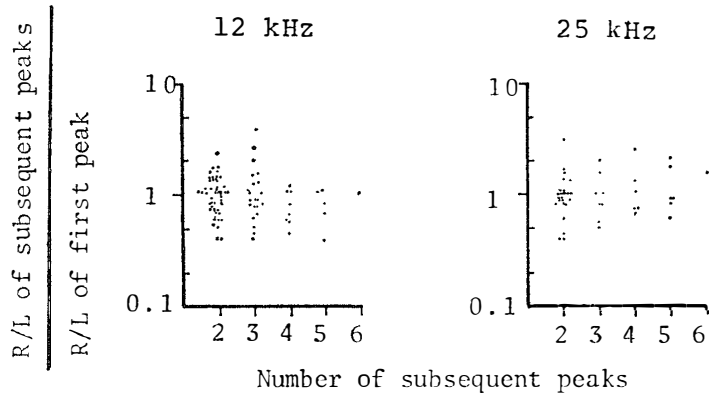

Fig. 31. Ratios of R/L on the subsequent peak to R/L on the first peak during the discrete VLF event appearing during not so much disturbed period with rather a short duration of about ten minutes.

observed polarization of the auroral hiss on the ground is expected to be affected by the ionospheric conditions. However, the facts given in the figures show that the wave couplings do not take place effectively and the polarization of the auroral hiss at VLF does not suffer any significant modifications in the lower ionosphere. Therefore, the polarization of the auroral hiss received on the ground is supposed to be nearly right-handed circular. The results of our measurement will be compared with the calculation of the limiting polarization by means of the full wave theory. Fig. 30 represents the occurrence probability of R/L of 12 kHz hiss for each range of flux density. It is found from this figure that the polarization does not relate to the energy flux of the hiss, either. Fig. 31 illustrates the ratios of R/L value of the subsequent peaks to the value of the first VLF peak for the discrete hiss event which appears in the moderately disturbed period with a rather short duration of about ten minutes. It is seen in the figure that the polarizations of the hiss subsequently received do not change markedly during the period of the event. This suggests that the wave normals are kept almost constant during the event, and it gives indirect evidence to the existence of field-aligned ducts in which the auroral hiss is trapped.

4. Discussion of the Observed Characteristics of the Polarization, Incidence Angle and Arriving Direction

4.1. Full wave calculation of the polarization and its comparison with the measurements

In this section, we study the polarization of auroral hiss downgoing through the auroral ionosphere by using the full wave method worked out by PITTEWAY and JESPERSEN (1966). The notations used in this section follow PITTEWAY's. For the sake of simplicity we treat only the properties of the propagation within the magnetic meridian plane. In the auroral ionosphere where the earth's magnetic field makes a small angle with the vertical direction, the dependence of the limiting polarization as well as the transmission coefficient on the azimuthal direction may be negligibly small.

The ionospheric model used for the numerical computations is drawn in Fig. 32. This electron density height distribution was observed on board the S-210 JA-9 rocket launched at Syowa Station at midnight on 12 December 1972, when the horizontal component of the geomagnetic field showed a moderate fluctuation of -290γ and the cosmic noise absorption was -1.3 dB and a nearly complete radio blackout occurred (MIYAZAKI, 1975). The colli-

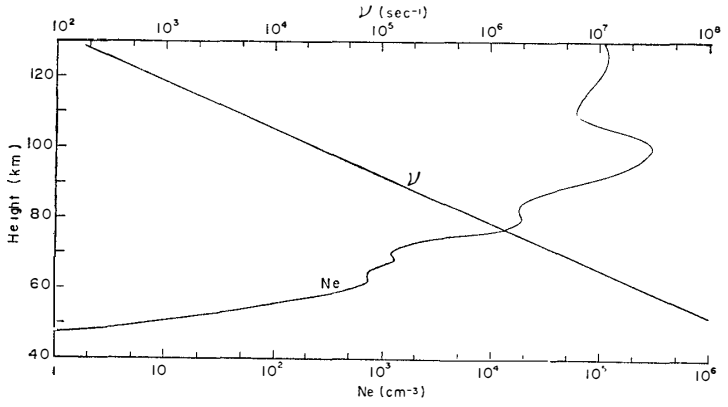

Fig. 32. The ionospheric model used for the full wave calculation.

sion frequency profile is based on rocket measurements made in the arctic D-region from Andoya in the north of Norway (JESPERSEN *et al.*, 1966). The calculations are made in the case of the geomagnetic latitude of 69.6° and the gyro-frequency there is taken to be 1.602 MHz. Fig. 33 shows the variation of the whistler transmission coefficient of downgoing whistler waves with exit angle as a function of frequency. The transmission coefficient is maximized for the exit angle parallel to the earth's magnetic field and becomes smaller as the exit angle departs from the field direction. Furthermore, it becomes smaller with increasing frequency and its rate of decrease with respect to exit angle is more enhanced for higher frequencies. The model of the ionosphere used here is the considerably disturbed night one with increased ionization in the lower height range. Wave coupling affecting the polarization is thought to occur more effectively in the lower ionosphere with increased ionization, so that we chose this considerably disturbed model in order to investigate the change in the polarization of the auroral hiss received on the ground during moderately disturbed periods. During the slightly disturbed periods, the transmission coefficients are greatly increased compared with the result in Fig. 33.

Figs. 34 and 35 show the limiting polarizations with which the downgoing whistler waves emerge into free space below the ionosphere. Fig. 34 shows the variation of $\tan^{-1}|a|$ with exit angle with a parameter of frequency, where 'a' indicates the ratio of perpendicular to parallel polarization in the electric vector. Fig. 35 gives the corresponding variation of arg (a) with exit angle. It is seen from these figures that the polarization is nearly right-handed circular at small exit angle or incident angles, but it departs from the circularity at larger angles. The tendency of the departure from circular polarization is more evident for lower frequencies such as 0.75 kHz.

There is a possibility that the ions in the lower ionosphere play a significant role in the limiting polarization as well as the transmission coefficient at 750 Hz, and so we have checked the ion effects. The ions are assumed to be singly charged and therefore, for charge neutrality the positive-ion concentration at any height is given by the sum of the electron and negative-ion concentrations. The negative- and positive-ion concentrations are conveniently introduced by the parameter, k, the ratio of negative-ion to electron concentrations. Thus, for any electron density (N), the corresponding negative-ion concentration (N_i^-) is kN, and that of positive ions (N_i^+) is $(k+1)N$ (THOMAS, 1969). The height variation of k adopted in the calculations represents a straight-line approximation of the variation deduced for daytime by COLE and PIERCE (1965). The ion-neutral collision frequency is taken from COLE and PIERCE (1965) and BANKS (1966). The value of the

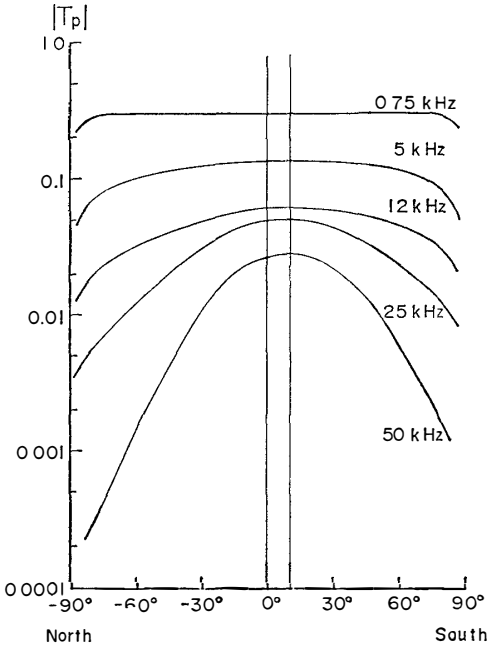

Fig. 33. Variation of whistler transmission coefficient with exit angle with a paramter of frequency. The inclination of the earth's magnetic field is taken to be 10.5°, with a gyrofrequency of 1.602 MHz. The vertical line indicates that the exit direction is parallel to the geomagnetic field.

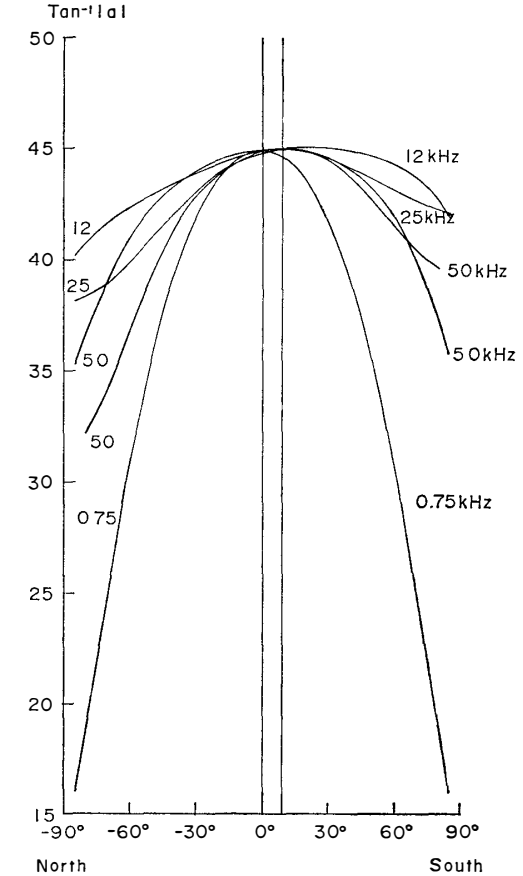

Fig. 34. Variation of $\tan^{-1}|a|$ with exit angle with a parameter of frequency.

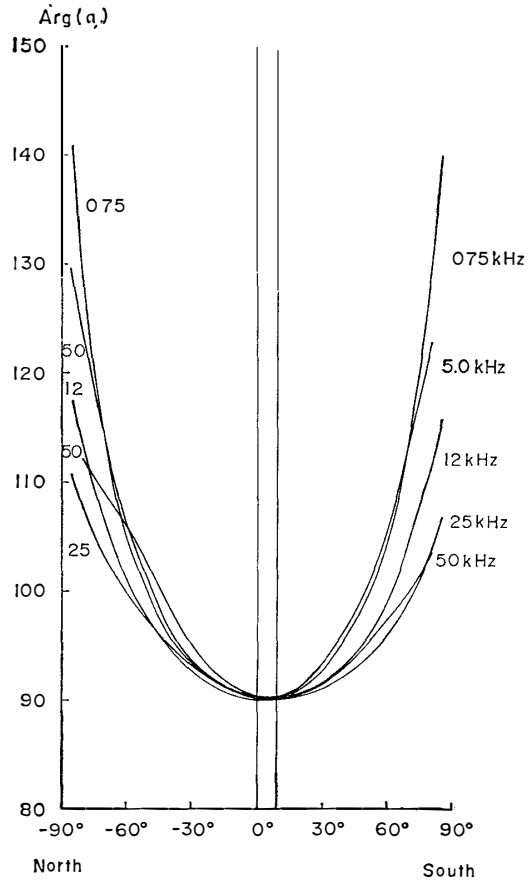

Fig. 35. Variation corresponding arg (a) with exit angle.

atomic mass unit of the ions has been adopted to be 30. Under these conditions, we have carried out the calculations of the limiting polarization and transmission coefficient at 750 Hz including the effects of ions. It is found, as a result, that the ions have no significant influences on the limiting polarization or on the transmission coefficient at 750 Hz over the whole range of exit angles.

4.2. Effect of waves from multiple directions on polarization records

When a single wave with right-handed circular polarization is received, the ratio of R- to L- components can be given by $R/L=(1+\cos i)/(1-\cos i)$. As was shown by the full wave studies in 4.1., the polarization of the down-going whistler wave is not completely circular, so that the R/L values are slightly different from the values for the complete circular polarization, but the differences are not so large as to affect the following discussion, with the exception of the case of 750 Hz, even when the wave coupling seems to occur through the lower ionosphere where the ionization is much enhanced by precipitating auroral particles. The result of the comparison of the R/L value based on the assumption of complete circular polarization with that calculated by the exact full wave method is presented in Table 1.

Table 1. The R/L values for the right-handed circularly polarized wave and the same values calculated by the full wave theory at the five specific frequencies with a parameter of incident angle.

Incident angle (deg.)	Right-handed circular polarization	Full wave treatment				
		750 Hz	5 kHz	12 kHz	25 kHz	50 kHz
0	infinite	infinite	446.8	446.5	364.4	275.6
10	130.6	67.2	112.7	133.9	123.1	123.1
20	32.2	17.4	27.5	32.9	30.3	29.7
30	13.9	7.6	11.7	13.7	12.6	12.2
60	3.0	1.8	2.5	2.8	2.7	2.6
80	1.4	1.10	1.25	1.35	1.36	1.33
90	1.0					

Impulsive auroral hiss with wide band frequency range is closely associated with the auroral break-up around the zenith as shown in 3.1. and, moreover, the results observed with our CRT method show that the incident angles are not so large. If we would explain the observed results on R/L values under the condition that a single wave with right-handed circular polarization is received, the incident angles must be, in general, quite large. However, on

this occasion the ionospheric transmission coefficient becomes smaller with increasing angle of incidence and this tendency is more pronounced for higher frequencies, as shown in Fig. 33. Moreover, there is little experimental evidence that energy in the VLF range could propagate over long distances (HELMS and TURTLE, 1964 ; HARANG, 1968). So, as a conclusion, we cannot reasonably explain the observed results of R/L values by the idea that a single wave with right-handed circular polarization is received in general.

VERSHININ (1970) has observed VLF hiss at stations in Siberia and found that the changing of direction of magnetic antenna orientation strongly affects the level of registered signal unless the source is just overhead of the observation point and the magnetic antenna oriented in geomagnetic NS has picked up the greatest output. Applying Fermat's principle to the plane ionosphere, MAEDA and KIMURA (1956) have demonstrated that a wave radiated in every direction into the lower ionosphere is focused into the magnetic meridian plane as it reaches the top of F layer. Auroral hiss whose energy is radiated along cones about the magnetic field line because of the symmetry of the medium, can be focused into the magnetic meridian plane by applying their result to auroral hiss propagating downward through the magnetosphere. Hence, the emergence of the auroral hiss into free space is mainly confined in the magnetic meridian plane. However, the auroral hiss is received when the ionosphere is moderately disturbed. So, it can also be supposed that the energy of focused auroral hiss is somewhat scattered out of the magnetic meridian plane by the irregularities in the auroral ionosphere. Therefore, we can easily suppose that the energy does not penetrate into free space in all direction but that the azimuthal direction of penetration is limited to a broad range around the magnetic meridian plane.

We now, therefore, consider the waves with right-handed circular polarization as coming from multiple directions in azimuth and incidence in order to explain our observed results reasonably. For the sake of simplicity of numerical studies, we assume that multiple waves with right-handed circular polarization are simultaneously received with equal magnitude of intensity. Then the ratio of R- to L-components of the received signal is given by

$$(R/L)=\left[\frac{\{\sum \cos i_n \sin(\theta_n-\alpha_n)+\sum \sin(\theta_n-\alpha_n)\}^2+\{\sum \cos i_n \cos(\theta_n-\alpha_n)+\sum \cos(\theta_n-\alpha_n)\}^2}{\{-\sum \cos i_n \sin(\theta_n+\alpha_n)+\sum \sin(\theta_n+\alpha_n)\}^2+\{\sum \cos i_n \cos(\theta_n+\alpha_n)-\sum \cos(\theta_n+\alpha_n)\}^2}\right]^{1/2}$$

where, θ_n is the azimuthal angle of the n-th wave, measured clockwise from the geographic north. i_n is the incident angle of the n-th wave and α_n is the phase difference given by $\omega t_n=\omega t+\alpha_n$, $\alpha_1=0$.

We can easily understand the following two cases from this equation. If incoherent waves from a single source, namely the same exit point of the ionosphere, are simultaneously received, R/L values are nearly equal to that for a single wave. Even if a number of waves are received from multiple azimuths, R/L values are nearly equal to that for the single wave only for the same incident angle.

Therefore, we will consider two or three waves with right-handed circular polarization and with equal intensity. It is assumed that the incident angle is different for each wave and the azimuthal angle is different or equal and that the phase of each wave is distributed completely at random. Fig. 36 shows the distribution of R/L values based on the aforementioned assumption of waves simultaneously received under the following conditions, numerically analyzed with the R/L equation.

(a) Two waves are simultaneously received. Case (1)
Incident angles : 30°, 50° ; 40°, 60° ; or 50°, 70°
Azimuthal angles :
0° : corresponding to two waves coming from geomagnetic north
−15°∼15° : corresponding to two waves coming from arbitrary directions within −15°∼15° about geomagnetic north
−30°∼30° : corresponding to two waves coming from arbitrary directions within −30°∼30° about geomagnetic north
all directions : corresponding to two waves with arbitrary angles of azimuth

(b) Three waves are simultaneously received. Case (2)
Incident angles : 30°, 40°, 50° ; 40°, 50°, 60° or 50°, 60°, 70°
Azimuthal angles : conditions similar to case (1).

It is suggested from the figure that the distributions in the case of two and three waves coming with not so large angles of incidence from the directions within a small range about geomagnetic NS are roughly similar to the observed results on R/L values shown in Fig. 22 and that the distributions for the waves coming from various directions do not coincide at all with the observed results. Therefore, the auroral hiss is thought to be the consequence of the sum of a few wave packets with not so large angles of incidence propagating roughly in the meridian plane.

However, a slight difference on the distribution of R/L values between the observations and our model calculation, may be caused by the simplicity or inadequancy of our model, one of which may be attributed to the assumption of the complete circular polarization at large incident angles of several tens of degrees, contrary to the full wave calculation results shown in Table 1 and Figs. 34 and 35. The R/L values of less than 1.0 and greater than

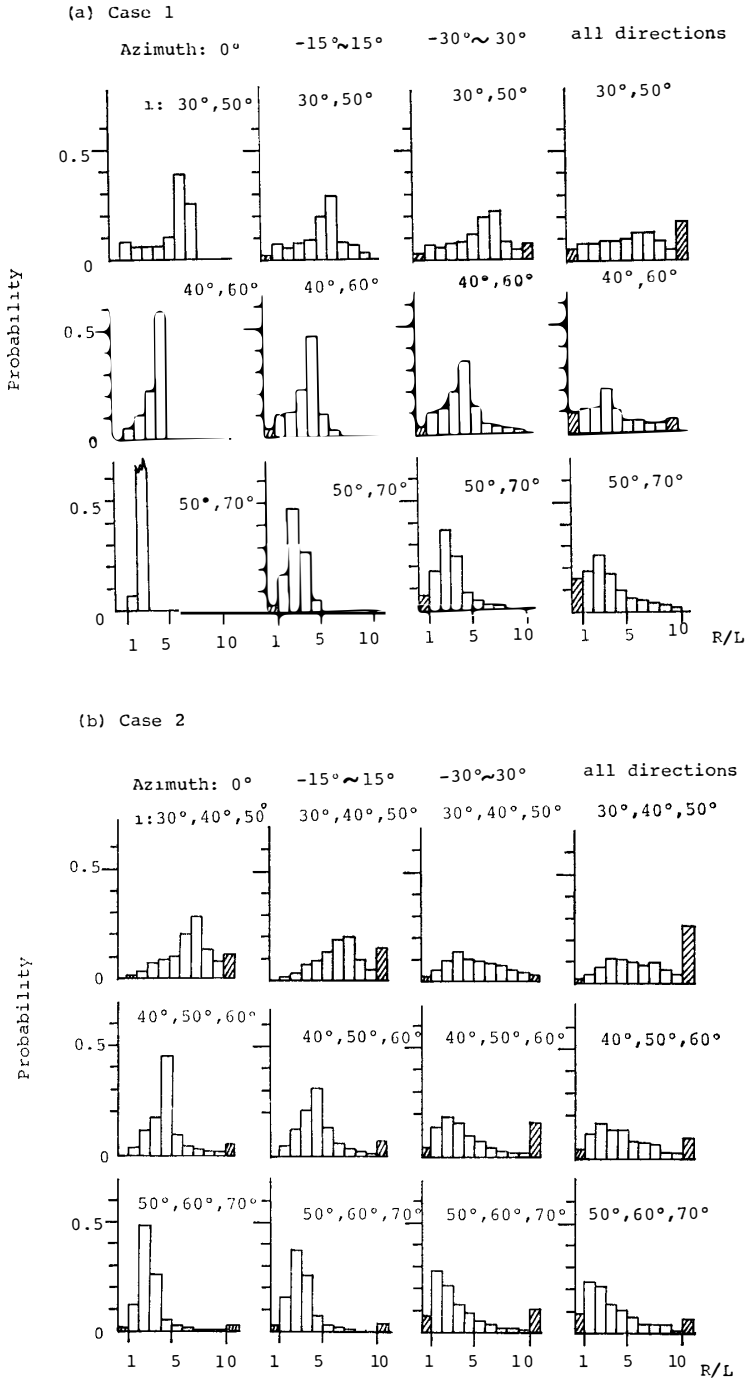

Fig. 36. Distribution of R/L values on the assumption that two or three waves with right-handed circular polarization and with equal amplitude are simultaneously received. The phase of each wave is taken to be distributed completely at random. The hatched regions represent the distribution probabilities of R/L less than unity or greater than or equal to 10.0. Fig. (a) refers to Case (1) and Fig. (b) Case (2) in the text.

or equal to 10.0 shown by hatched regions in Fig. 36, are given by the R/L equation under the condition that the phase differences are large and the waves are approximately in anti-phase. The signal could not, practically, be observed because of its faint intensity under this condition.

It is seen in Fig. 24 that the polarizations at 25 and 50 kHz are much more nearly linear than those at 12 kHz and some of them are left-handed. This may be accounted for in terms of the insufficient trapping of the energy within the field aligned duct and within the magnetic meridian plane of the higher frequencies and the resultant multiple directions of azimuth and incidence. As was shown in Fig. 26, ELF hiss at 750 Hz is found to be slightly right-hand polarized. The transmission coefficient at this frequency is relatively constant with respect to the exit angle with the exception of nearly 90° of incidence, as is presented in Fig. 33. Moreover, the polarization at 750 Hz approaches to linear with larger exit angles. For example, the R/L value is 1.8 at the exit angle or incident angle of 60°, in contrast with the R/L value of 3.3 for complete circular polarization. Judging from these facts, it may be reasonable that the observed polarization of ELF hiss is slightly right-handed and so the incident angle of ELF hiss is very large.

4.3. A device for the direction finding of noisy signals and its application to the study of auroral hiss

The direction finding (DF) method carried out at Syowa during the period of 1967 to 1970 is, strictly speaking, useful only for monochromatic waves. A new DF method measuring the direction of energy flow (TSURUDA and HAYASHI, 1975) has a couple of merits that the measuring accuracy is independent of the ground conductivity and the method is useful even for the incoherent signals if they come from a single source.

However, the signal of auroral hiss received on the ground seems to be in most cases, composed of several components downcoming from multiple directions. So, it is very significant to investigate whether the received signal is coherent or not, and whether it consists of components downcoming from multiple directions or is an isolated burst. For this purpose, we have an observing plan to measure the auto-correlation of the signal at a point and the cross-correlation between the signals received at two observing points. Our new DF system of auroral hiss is based on the measurement of the time difference with which the same wave form of auroral hiss at a certain frequency reaches the two observing points. The time difference of arrival can be confirmed by multipling the signal by the other one with shifting of the delay time and by detecting the best-correlation coefficient at a certain time.

When we carry out the DF of noisy signals such as auroral hiss, the

obtained results of the direction should be carefully examined. If the cross-correlation coefficient is high, the signal is thought to be an isolated burst or have a dominant component in magnitude and this DF system is useful.

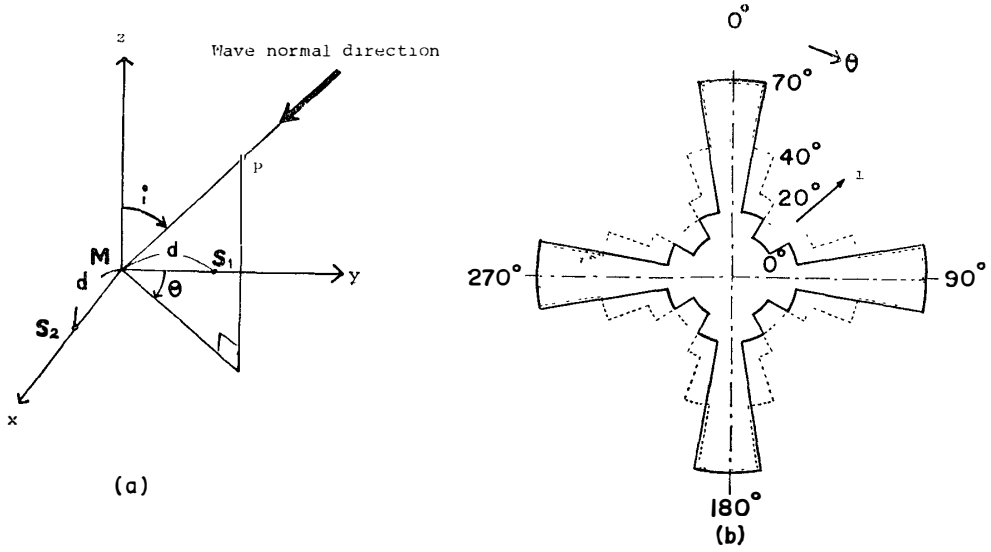

Fig. 37. (*a*) *Principle of the proposed new DF system based on the measurement of time difference at three observing points. The arrow shows the down-going plane wave whose incident and arriving angles are given by i and 0.*
(*b*) *The time resolution of 1 μsec is required to satisfy the measuring accuracy of ten degrees in azimuth and incidence, along the solid curve, assuming a downcoming plane wave and the distance of 20 km between the master station to each slave station. A more severe time resolution is necessary to satisfy the same measuring accuracy, inside the region bounded by the solid line. Outside the region, the condition of the time resolution required becomes soft. The broken line corresponds to the condition of 2 μsec. The azimuthal angle of 0 is measured clockwise from the Y-axis and the incident angle of i is represented as the radial distance.*

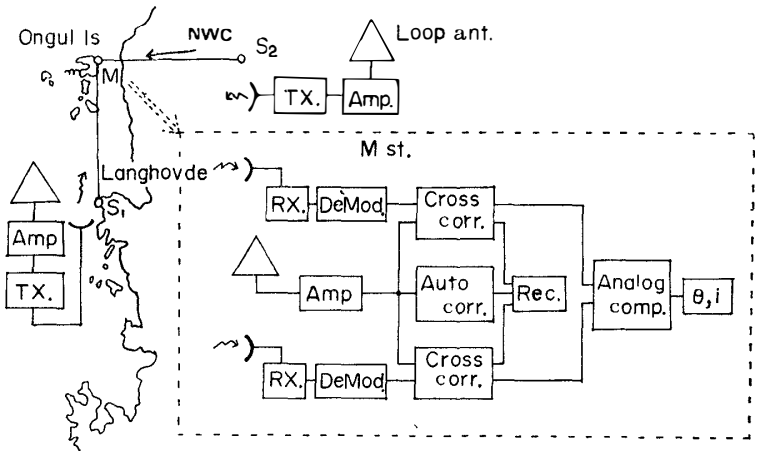

Fig. 38. Configuration of the three observing stations and block diagram of the new DF system.

To the contrary, a very poor coefficient will give the warning that DF of the received signal cannot be reasonably done at all.

Considering the facts of about 2 orders shortening of the calculated intensity of auroral hiss below the observations (LIM and LAASPERE, 1972; TAYLOR and SHAWHAN, 1974) and a threshold low-energy electron flux below which VLF hiss is not observed (GURNETT and FRANK, 1972), it has been indicated that a coherent plasma instability mechanism is partially involved in the generation of auroral hiss. Therefore, it seems very significant to investigate the coherency of the signal.

Using the time differences of arrival between the signals received at three observing points situated at intervals of about 20 km as shown in Fig. 37 (a), the azimuthal angle (θ) and the incident angle (i) can be measured. For simplicity, we arrange these observing points to be at right angles and at the same interval (d) of about 20 km. Here, we assume that the received signal is a plane wave. As the interval of the distance (d) is longer, the measuring accuracy of the time becomes better but the assumption of the plane wave becomes worse and moreover the maintenance of the telemetry and other systems becomes more difficult. The time differences of t_1 and t_2 between the master station (M) and the first slave station (S_1) and M and S_2 stations are given by

$$t_1=\frac{d}{c}\cos\theta\cdot\sin i,\quad t_2=\frac{d}{c}\sin\theta\cdot\sin i,\quad \text{where } c \text{ is the speed of light.}$$

Hence, $\tan\theta=t_2/t_1$, $\sin i=\frac{c}{d}\sqrt{t_1^2+t_2^2}$

The time resolution is required to be one microsecond in order to keep a measuring accuracy of ten degrees in azimuth and incidence, with the exception of the direction close to the base line, as shown in Fig. 37 (b). Fig. 38 shows the configuration of the three observing stations of the master station (M) at Syowa in East Ongul Island and two slave stations (S_1, S_2) at Langhovde and on the iced slope of Antarctica. The block diagram of our DF apparatus as it is roughly planned is also illustrated in Fig. 38. Auroral hiss is received at each observing point by a loop aerial and the received signal is led to a wide band amplifier of which the gain is flat in the frequency range of $\sim$0.1 to $\sim$100 kHz. The wide band signal is transmitted from each slave station to the main station at Syowa. The transmission antenna is of the parabolic or helical type. The frequency of the carrier wave will be chosen to be about 2 GHz with a band width of about 1 MHz. The component at a certain frequency, for example at $\sim$20 kHz, is first selected from the wide band signal received at the main station through the circuit detecting the arriving time difference. And then its azimuthal and incident

angles can be computed.

As our DF system is based on measuring the time differences of arrival of the same wave form at three observing points, it is important to keep equally the phase characteristic of each total observing system. Therefore, the phase adjustment of the total system should be carefully made by using NWC communication wave of 22.3 kHz of which the azimuthal direction is known.

PART II. MORPHOLOGY OF AURORAL HISS AND ITS COMPARISON WITH THAT OF LOW-LATITUDE HISS

1. Introduction

As was shown in 3.1. in Part I, the VLF emissions in the auroral regions are closely associated with auroral display (MARTIN *et al.*, 1961 ; MOROZUMI and HELLIWELL, 1966) and are named auroral hiss. Auroral hiss is considered to be a manifestation of polar substorms (MOROZUMI and HELLIWELL, 1966 ; AKASOFU, 1968 ; HAYAKAWA *et al.*, 1975), and JØRGENSEN (1968) has suggested that it is generated by incoherent Cerenkov radiation from precipitating low-energy electrons of ≤ 1 keV. However, the recent works by LIM and LAASPERE (1972) and TAYLOR and SHAWHAN (1974) have shown that the observed intensity of auroral hiss is still greater by about 2 orders of magnitude than the intensity calculated on the basis of the realistic plasma parameters. GURNETT and FRANK(1972) have, then, obtained a direct verification of the association between the auroral hiss and the intense fluxes of electrons with energies of the order of 100 eV to several keV. Furthermore, they have found a threshold effect in the generation of auroral hiss ; that is, there is a threshold low-energy electron flux below which VLF hiss is not observed. Such a threshold effect as well as the shortening of the calculated intensity below the observations has led them to postulate that a coherent plasma instability mechanism is partially involved in the generation of auroral hiss.

JØRGENSEN (1966) has summarized the observations of hiss in the frequency range 4–9 kHz at thirteen stations in the world and found that the intensity of hiss is relatively constant in the auroral zone, while it decreases with decreasing latitude outside the auroral zone. The obtained rate of decrease of maximum spectral density with latitude of about 10 dB / 1000 km and satellite evidence of correlation of auroral hiss with particle precipitation have led him to conclude that VLF hiss is exclusively generated in the auroral

zone and it propagates to lower latitude via waveguide mode propagation below the ionosphere, resulting in low-latitude hiss. Since his work, the low-latitude hiss observed on the ground is thought to be the consequence of waveguide mode propagation of auroral hiss (RAO *et al.*, 1972). However, there is little direct evidence that auroral hiss propagates over long distances (HELMS and TURTLE, 1964 ; HARANG, 1968).

In addition to auroral hiss, HARANG (1968) has found a new type of VLF hiss named ' low-latitude ' type hiss which shows features significantly different from auroral hiss. This low-latitude hiss is characterized by the fact that it appears at stations of lower latitudes than the auroral zone during and after great geomagnetic disturbances and it is usually not recorded close the auroral zone. VERSHININ (1970) has also observed hiss belonging to the category of low-latitude hiss.

This middle- or low-latitude VLF hiss has recently been found to be clearly different from auroral hiss. Observations made both at ground stations (JØRGENSEN, 1968 ; NISHINO and TANAKA, 1969a ; TANAKA, 1972 ; HAYAKAWA *et al.*, 1975) and by satellite experiments (LAASPERE *et al.*, 1971 ; HUGHES and KAISER, 1971 ; KAISER, 1972 ; GURNETT and FRANK, 1972 ; JAMES, 1973 ; LAASPERE and JOHNSON, 1973) have shown that auroral hiss is a broad band phenomenon that extends from frequencies of the order of a few kHz to half a MHz. This is totally different from the band-limited or narrow-banded VLF hiss observed at low-latitude ground stations (LAASPERE *et al.*, 1964 ; HAYAKAWA *et al.*, 1975) and by satellites near the equatorial plane (BURTIS, 1969).

However, a clear understanding of the distinction in characteristics between auroral and low-latitude VLF hiss has not been obtained up to date. The purpose of this part of the paper is, therefore, to make an extensive comparison of features between auroral and low-latitude VLF hiss, from the morphological standpoint, using the data of auroral and low-latitude VLF hiss based on the observations at Syowa Station in Antarctica during the period of 1967 to 1968 and at MOSHIRI (geomag. lat. 34.3°) in Japan during the period of 1964 to 1968.

2. Morphology of Auroral Hiss

The diurnal variation of the occurrence rate of auroral hiss at 12 kHz was already shown in Fig. 10. The statistical results of the diurnal variation of the normalized occurrence at four specific frequencies of 5, 8, 12 and 25 kHz are given in Fig. 39. An arrow in the figure indicates the time of magnetic midnight. It is found from this figure that auroral hiss is predominantly observed during a limited local time period around midnight, *i. e.* 2000 h to 0400 h LT for all the relevant frequencies, as already mentioned in 3.1. These results are in good agreement with those of earlier works by HARANG and LARSEN (1965), JØRGENSEN (1968) and HARANG (1968). In addition to the occurrence of hiss around midnight, the satellite observations have demonstrated an additional maximum in hiss intensity in the afternoon at approximately 1400 h LT (GURNETT, 1966 ; MCEWEN and BARRINGTON, 1967 ; BULLOUGH *et al.*, 1969 ; LAASPERE *et al.*, 1971 ; HUGHES and KAISER, 1971 ; KAISER 1972). The disappearance of afternoon hiss on the ground is probably due to the enhanced

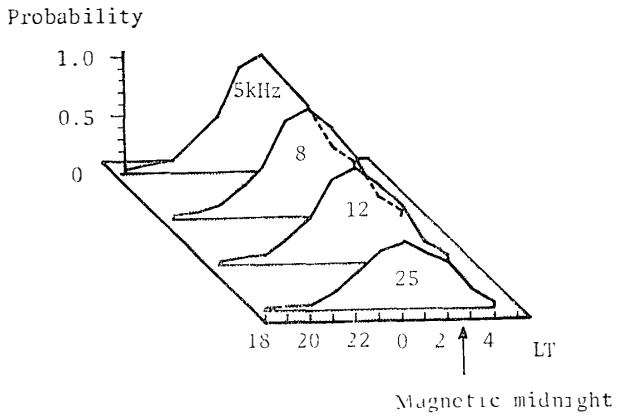

Fig. 39. Local time dependence of the relative occurrence number to the maximum occurrence at 5 kHz in 1968. An arrow indicates the time of magnetic midnight.

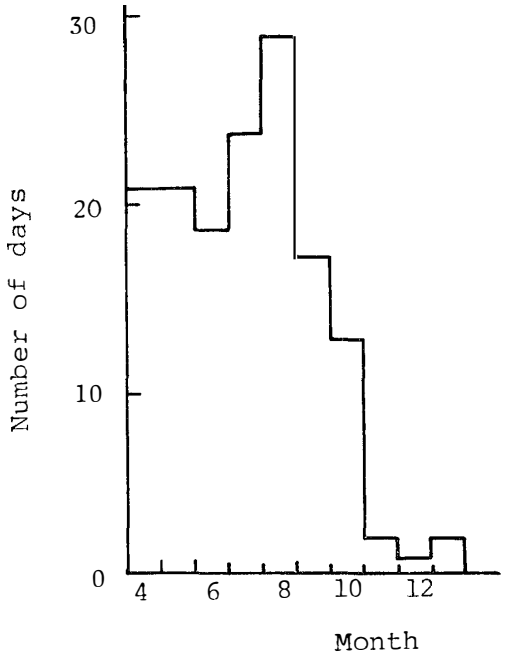

Fig. 40. Seasonal variation of the occurrence of auroral hiss in 1967.

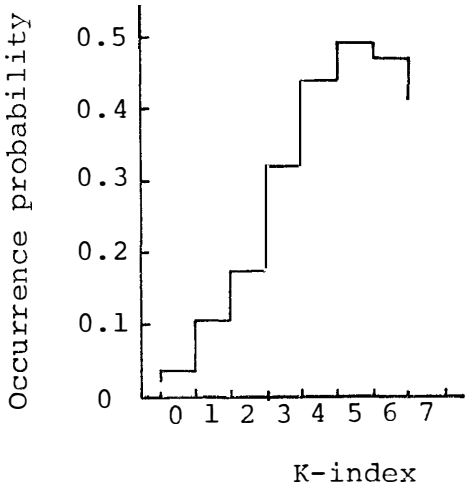

Fig. 41. Dependence of the occurrence probability on magnetic activity in 1968.

absorption of VLF wave in the afternoon or due to the difference in S/N ratio. The peak intensity of auroral hiss is found to follow the auroral oval (RUSSEL, 1972 ; KAISER, 1972). The zone of hiss appears to coincide with the precipitation zone of soft electrons (~1 keV) (HARTZ and BRICE, 1967 ; PAULIKAS, 1971), which had led JØRGENSEN (1968) to present the reasonable hypothesis that auroral hiss may be generated by incoherent Cerenkov radiation from incoming auroral electrons with energies of the order of 1 keV. But recent studies by LIM and LAASPERE (1972), GURNETT and FRANK (1972) and TAYLOR and SHAWHAN (1974) have shown that the particle fluxes at night are certainly too low to explain the observed intensity and they have suggested that a coherent plasma instability mechanism is involved in auroral hiss generation.

The seasonal variation of occurrence rate of hiss at 12 kHz is shown in Fig. 40. It is found that auroral hiss tends to appear predominately in winter season. This seasonal dependence can be attributed to the seasonal effect of ionospheric absorption, as suggested by HARANG and HAUGE (1965).

It is interesting to investigate the association of auroral hiss with the geomagnetic activity. Fig. 41 shows the occurrence probability of auroral hiss at 12 kHz versus K-index at Syowa. From this figure it is seen that the occurrence probability of auroral hiss has a positive correlation with geomagnetic activity during slightly and moderately disturbed periods and it decreases with further enhancement of geomagnetic activity. The index of magnetic activity

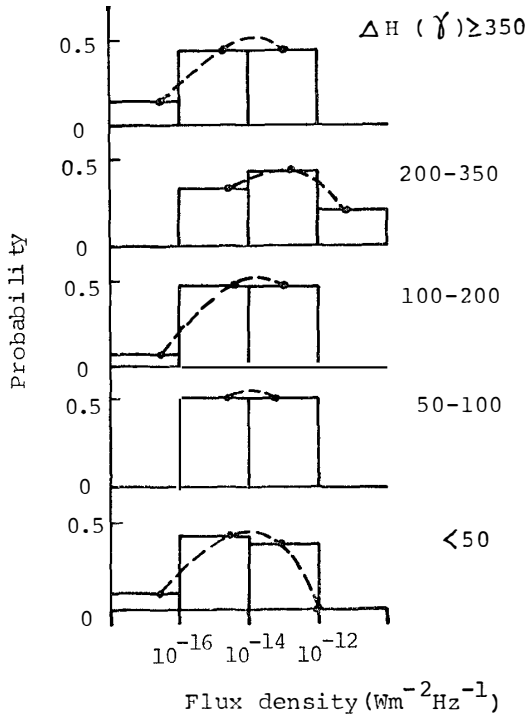

Fig. 42. Occurrence probability of VLF hiss at 12 kHz as a function of flux density for five degrees of geomagnetic activity in 1968.

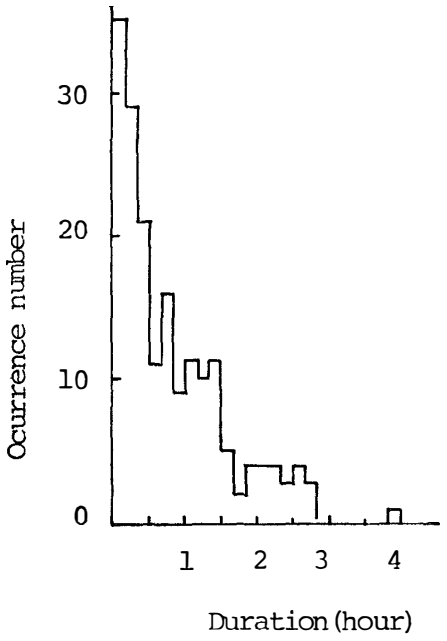

Fig. 43. Occurrence histogram of the duration of auroral hiss in 1967.

has a good correlation with precipitating electrons in the auroral zone (KUCK, 1970). The ionization in the lower ionosphere is greatly enhanced during severe geomagnetic activity, which then results in the depleted occurrence of VLF emissions (ECKLUND *et al.*, 1965), being consistent with the result of Fig. 41. Fig. 42 shows the occurrence probability of auroral hiss at 12 kHz against the flux density for each range of geomagnetic activity. This figure shows that the intensity of hiss increases till the geomagnetic activity increases to a critical value and it decreases when the activity exceeds such a critical value. This tendency seems to be identical to that for the association of occurrence rate with geomagnetic activity.

Fig. 43 shows the occurrence histogram of the duration of auroral hiss at 12 kHz. It is clear that the duration of auroral hiss is predominantly of the order of less than one hour. This duration is of the same order as the duration of polar substorms (AKASOFU, 1968) and hence auroral hiss can be considered to be a temporally localized phenomenon. Hiss with a duration of more than a few hours is seldom observed. Of course, the duration of auroral hiss shows a dependence on local time and it has a close association

with the development of polar substorms.

The most interesting characteristic of the frequency spectrum is the relation of hiss band to geomagnetic activity. When the geomagnetic activity is enhanced during moderately disturbed conditions, the frequency spectrum of hiss becomes very wide, that is, upper cutoff frequency extends up to more than 100 kHz (DOWDEN, 1960 ; JØRGENSEN, 1968 ; TANAKA, 1972), while the duration becomes short, as shown in Figs. 44 and 45. The dependence of the duration and the frequency spectrum of auroral hiss on geomagnetic activity was already outlined in 3.1. in Part I.

The intensity of auroral hiss observed on the ground is typically of the order of $\sim 10^{-14}$ W / m^2 / Hz (JØRGENSEN, 1968 ; TANAKA, 1972). While, the maximum hiss intensity measured on board the satellites is about 10^{-12} W / m^2 / Hz (GURNETT, 1966 ; RUSSELL, 1972 ; HUGHES and KAISER, 1972), being higher by two orders of magnitude than that observed on the ground. This may result from total as well as partial reflections in the ionosphere (THOMAS and SMEATHERS, 1971), ionospheric absorption (ONDOH, 1963 ; HAYAKAWA and OHTSU, 1972) and divergence in space after penetration through the ionosphere.

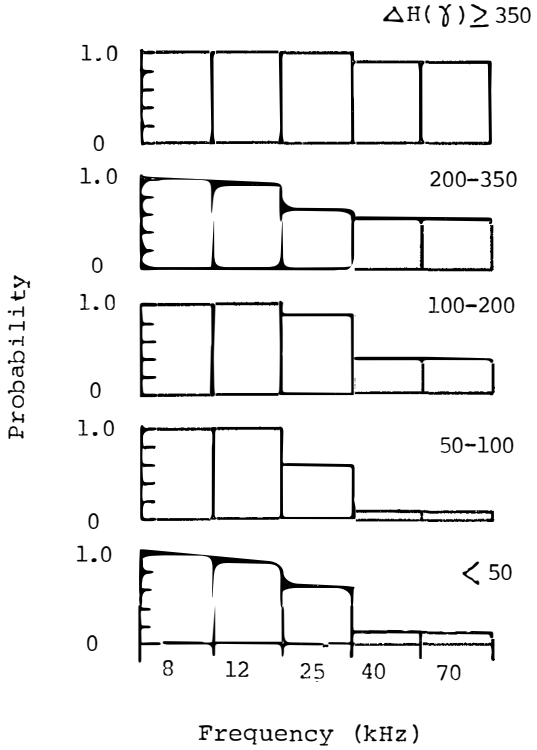

Fig. 44. Frequency dependence of the relative occurrence number to the occurrence at 5 kHz for various degrees of geomagnetic activity in 1968.

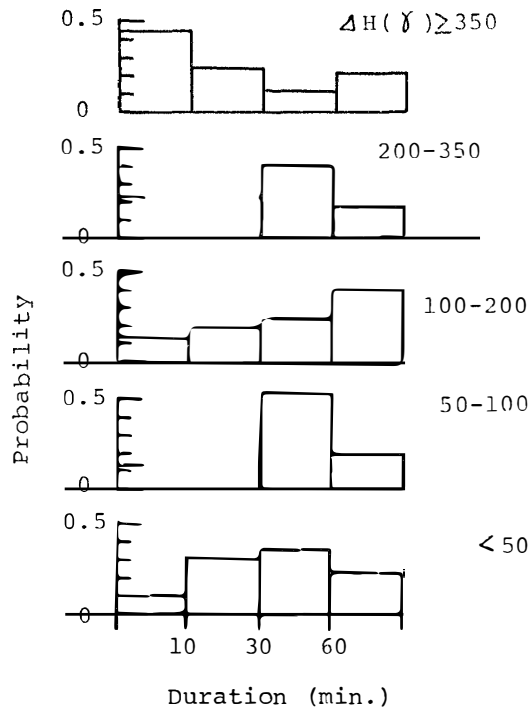

Fig. 45. Occurrence probability of the duration at 12 kHz versus geomagnetic activity in 1968.

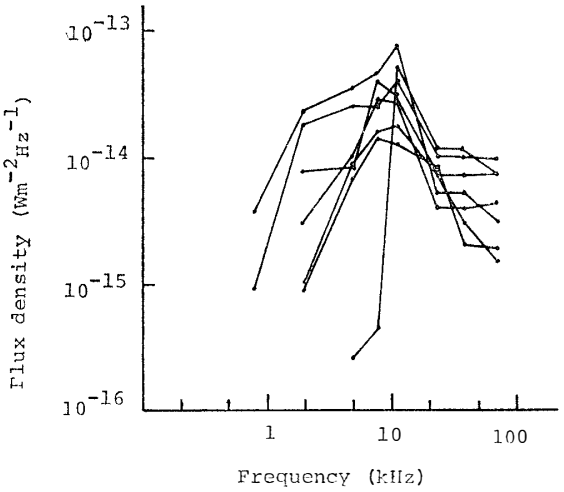

Fig. 46. Frequency spectra of auroral hiss based on seven hiss events in 1968.

The frequency spectrum of hiss intensity is illustrated in Fig. 46 which is based on seven hiss events. Fig. 47 shows the occurrence probability of hiss as a function of flux density at five specific frequencies of 2, 5, 8, 12 and 25 kHz. These figures indicate that the maximum intensity takes place at frequencies of around 10 kHz, being in good agreement with the previous results of JØRGENSEN (1968).

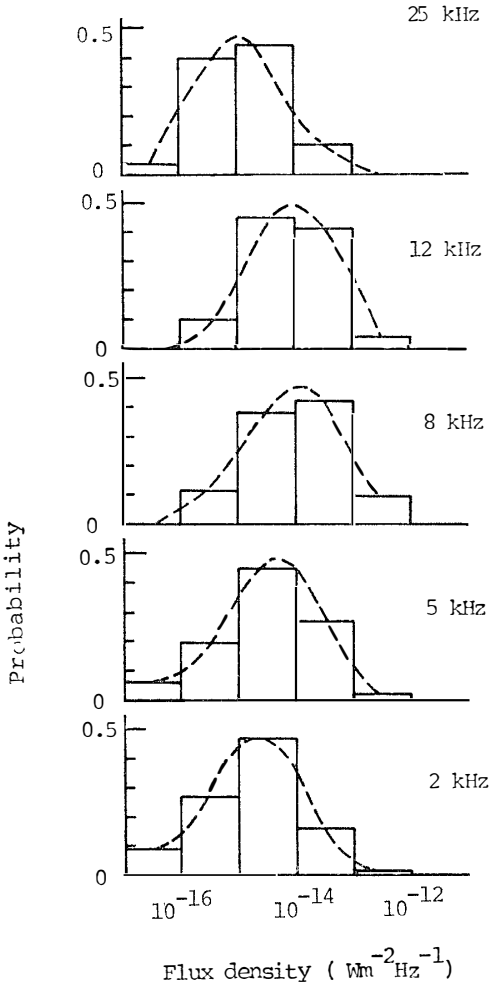

Fig. 47. Occurrence probability of VLF hiss events as a function of flux density at five frequencies based on the data in 1968.

3. Morphology of Low-Latitude VLF Hiss

The morphological features of low-latitude VLF hiss observed at Moshiri are discussed in comparison with those of auroral hiss.

The association of low-latitude VLF hiss with geomagnetic activity seems to be distinctly different from that of auroral hiss. Fig. 48 illustrates the occurrence probability of low-latitude hiss at 5 kHz versus geomagnetic activity. The daily sum of K_p index is used as the measure of geomagnetic activity. It is clear from the figure that the occurrence probability of low-latitude hiss increases with increasing $\sum K_p$. In particular, we can expect a surprisingly high value of $\sim$0.9 in occurrence probability for great geomagnetic storms whose $\sum K_p$ exceed 40. The hiss appearing in a high probability during severe geomagnetic storms differs essentially from auroral hiss which occur

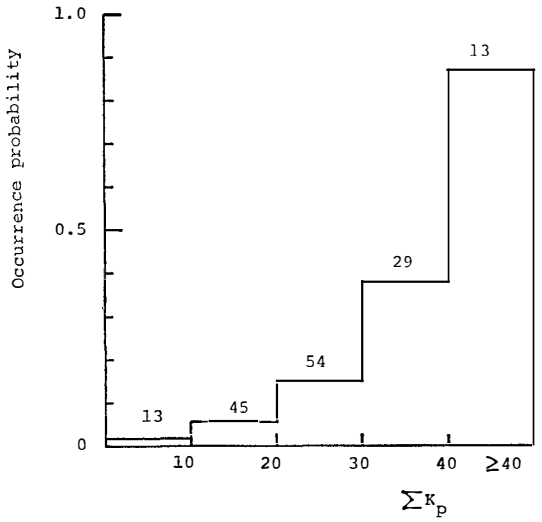

Fig. 48. $\sum K_p$ dependence of low-latitude VLF hiss observed at Moshiri Station. The value on the rectangle means the number of events for each $\sum K_p$ range.

during moderately disturbed conditions. Fifty six percent of the total VLF hiss observed at Moshiri in the period of January 1964 to December 1968 were associated with worldwide geomagnetic storms. We call these hiss closely correlated with geomagnetic storms 'storm-time hiss', while the remaining hiss is named 'quiet-time hiss'. LAASPERE *et al.* (1964) have suggested that VLF emissions at middle latitudes are essentially geomagnetic storm-time phenomena.

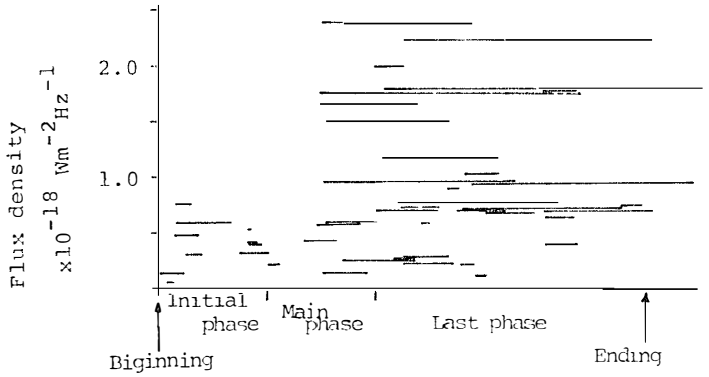

Fig. 49. The delay time of hiss behind storm commencement versus the maximum intensity of hiss. The duration of hiss is normalized to the length of each phase of the relevant storm. The relative length of each phase is drawn based on the average duration of each phase for 27 geomagnetic storms.

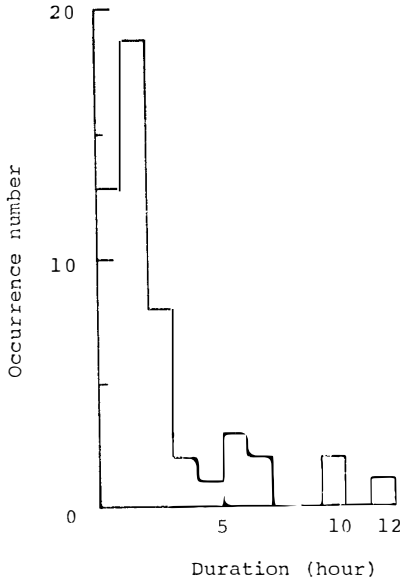

Fig. 50. Occurrence histogram of the duration of low-latitude hiss.

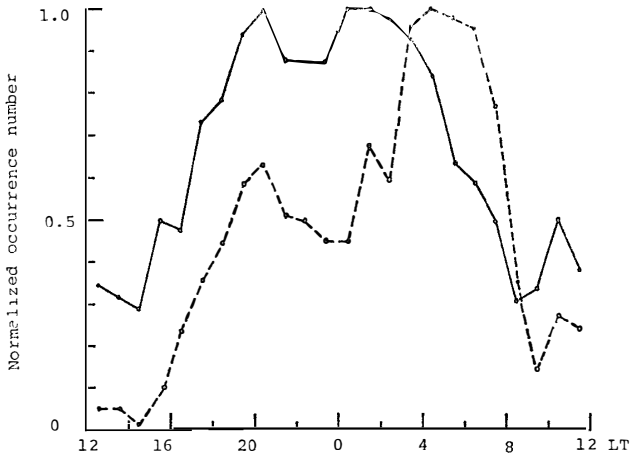

Fig. 51. Diurnal variation of occurrence rate of low-latitude VLF hiss associated with magnetic storms (full line) and not associated with storms (broken line).

Quiet-time hiss observed at Moshiri may belong to the category of equatorial hiss (GURNETT, 1968; LAASPERE *et al.*, 1971) or low-latitude hiss (BULLOUGH *et al.*, 1974). Of the two types, the storm-time hiss seems to be greater importance in relation to magnetospheric storms.

Fig. 49 shows the temporal variation and duration of the storm-time hiss. For each particular geomagnetic storm the duration of each of the initial, main and recovery phases is normalized to the corresponding mean duration depicted in the graph. It is seen from Fig. 49 that most of storm-time VLF hiss tend to occur during the period from the latter part of the main phase to the recovery phase and this coincidences with the results of HARANG (1968). The intensity of storm-time hiss is of the order 10^{-18}W/m^2/Hz (IWAI *et al.*, 1964) as seen from Fig. 49. This value holds for quiet-time hiss.

The duration of low-latitude VLF hiss during quiet- as well as storm-time is shown in Fig. 50 which illustrates the occurrence histogram of duration. In the case of auroral hiss in Fig. 43, the maximum duration is about 3 hours. In contrast, a lot of low-latitude VLF hiss are long-lasting and their duration extends, on some occasions, to over five hours.

However, there appears no significant correlation of the intensity of the hiss with the magnitude of the geomagnetic activity. This may be due to the difference in the energies between the energetic particles of the order of 100 keV mainly attributable to the DR field and the particles generating the hiss, or due to the complicated propagation conditions in the magnetosphere and below the ionosphere, which are probably caused by the greater distance of the generation region of the hiss from the observation point on the ground.

Fig. 51 shows the diurnal variations of occurrence rate of low-latitude hiss associated with and not associated with geomagnetic storms. In the figure the maximum occurrence rate at a certain time is normalized to unity. The hiss not associated with geomagnetic storms corresponds to quiet-time hiss and its diurnal variation consists of a pronounced peak at $\sim$5 h LT and a subsidiary one at 20 h LT. The remarkable peak at $\sim$5 h LT is found to coincide with the peak in occurrence rate of low-latitude whistlers (OHTSU *et al.*, 1963) and this may suggest that the diurnal variation in Fig. 51 may be, in most parts, from ionospheric absorption. The present diurnal pattern of quiet-time hiss based on ground observations is found to be in good accord with the satellite result (KAISER, 1972). But the origin of quiet-time hiss is not well known and needs further investigation making use of correlated study based on ground and satellite observations. We turn to the discussion of storm-time low-latitude hiss which is of greater significance in relation to magnetospheric consequences. It is reasonable to regard the diurnal variation of storm-time hiss as being composed of an evening peak around 20 h LT

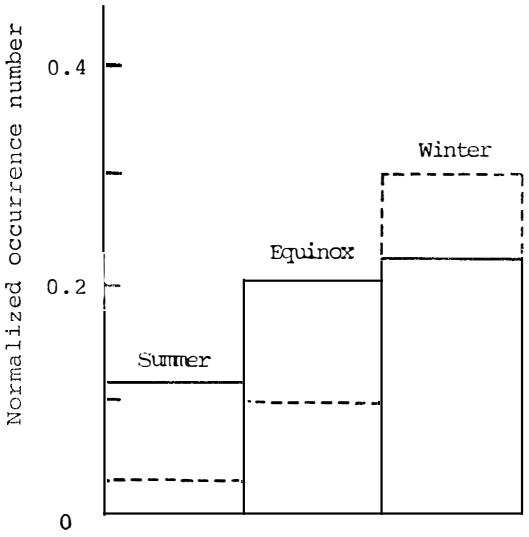

Fig. 52. Seasonal variation of the occurrence rate of storm-time (full line) and quiet-time hiss (broken line).

(we call 'evening hiss') and a post midnight one around 2 h LT ('morning hiss'). Earlier work by ELLIS (1959) has given strong support to such a two peak structure in diurnal variation of middle-latitude VLF hiss as mentioned above. In his paper such evening and morning peaks in occurrence pattern are much more well-isolated and the occurence peak of evening hiss occurs around 18h LT. The evening occurrence of hiss is of the same kind as that reported by VERSHININ (1970), who has found that the generation region of evening hiss is located inside the plasmapause. The appearance of hiss in the morning is closely correlated with D(day)-type hiss observed at lower latitudes by HARANG (1968). We have obtained results verifying the aforementioned two peaks from the recent studies based on the VLF observations on board the Ariel 3 satellite as well as on the ground during the severe geomagnetic storm of May 25–27, 1967 (BULLOUGH *et al.*, 1969b; TULUNAY and HUGHES, 1973 ; HAYAKAWA *et al.*, 1975).

Fig. 52 illustrates the seasonal variation of quiet-time and storm-time hiss. The broken line refers to the case of quiet-time hiss, the full line storm-time hiss. This figure shows that the seasonal variation of quiet-time hiss is wholly controlled by the difference of ionospheric absorption with season. On the other hand, the storm-time hiss shows less seasonal dependence, which indicates the more predominant effect of generation source compared to that of ionospheric absorption.

The frequency spectra of quiet- as well as storm-time low-latitude hiss show distinct differences from those of auroral hiss. That is to say, the low-latitude

VLF hiss always occurs within a relatively narrow frequency band. Its center frequency is found to lie usually in the frequency range 4–6 kHz and its bandwidth is about 2 kHz. On some occasions the upper frequency limit extends to as high as 8 kHz. According to recent work by LIKHTER *et al.* (1973), the VLF emission spectrum during geomagnetic storm has two maxima, one at 6 kHz and the other below 1 kHz. This satellite result is likely to be in good agreement with our ground observations.

4. Correlation of Auroral and Low-Latitude VLF Hiss with Polar Substorm and Worldwide Storms

Auroral VLF hiss appears predominantly during evening to post-midnight, as was seen in Fig. 39. The close relationship of this occurrence of hiss zone with the diurnal pattern of auroral precipitating electrons (JØRGENSEN, 1968 ; RUSSELL *et al.*, 1972) has led JØRGENSEN (1968) and LIM and LAASPERE (1972) to hypothesize that auroral hiss may be generated by incoming or precipitating auroral electrons during polar substorms. This idea is supported by the correlated observation of auroral hiss and soft electrons onboard satellites (FRITZ and GURNETT, 1965 ; JØRGENSEN, 1968 ; GURNETT and FRANK, 1972). Then auroral hiss can be considered to be only a manifestation of polar substorms which occur intermittently and impulsively with life times on the order of 1–3 hours (AKASOFU, 1968). The short duration of auroral hiss probably results from the short life time of polar substorms. MOROZUMI and HELLIWELL (1968) have classified the nighttime sequence of VLF hiss occurrence into three phases N1, N2 and N3 from comparison of VLF emissions with other geophysical phenomena. The N1 phase before midnight is characterized by the appearance of steady hiss and diffuse or arc aurora. While, the N2 phase, when impulsive hiss bursts occur almost simultaneously with a sudden increase in brightness of aurora, pi bursts and a sharp oneset of cosmic noise absorption, is interpreted as the expansion phase onset of a substorm in accordance with the recent concept of magnetospheric substorms (AKASOFU, 1968). And the N3 phase is the post-break-up phase of aurora. Generally speaking, auroral hiss tends to occur during moderate geomagnetic activity, not during severe geomagnetic activity. This is likely to be due to the absorption of VLF emissions caused by the increase in ionization of the lower ionosphere during severe geomagnetic activity. As is clearly seen from Fig. 48, low-latitude VLF hiss can be divided into two types. One is the hiss closely correlated with worldwide geomagnetic storms (storm-time hiss)

and the other is not associated with storms (quiet-time hiss). The first reliable report has been recently made of ground reception of low-latitude VLF hiss during geomagnetically quiet conditions (HAYAKAWA *et al.*, 1975). The origin or mechanism of quiet-time low-latitude VLF hiss has not been well understood. More recently BULLOUGH *et al.* (1974) have found, by making use of Ariel satellite data, low-latitude zones of VLF hiss which appear around the invariant latitudes of 30° and which is quite similar to the zone of low-energy electron flux (KNUDSEN, 1968). They have speculated, therefore, that its generation is due to the Cerenkov mechanism by such low energy electrons. But, further investigation should be made of the quiet-time hiss. The storm-time low-latitude hiss being of greater significance in relation to geomagnetic storms, shows distinct differences of the narrow band phenomenon and a close correlation with severe worldwide geomagnetic storms, as opposed to auroral hiss

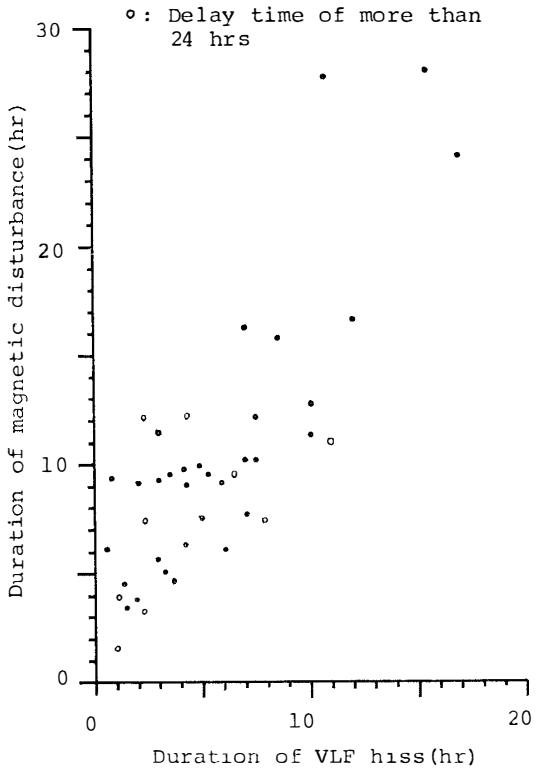

Fig. 53. Relation between VLF hiss duration and the geomagnetic disturbance duration: the latter is defined as the length of the time interval in which the H-component geomagnetic deviation exceeds half of the maximum deviation from the beginning of main phase.

which is a broad band phenomenon and is closely associated with the moderate activity of polar substorms.

We now examine in more detail the storm-time low-latitude hiss. Fig. 53 shows a positive correlation between the duration of hiss and the duration of geomagnetic disturbances. The geomagnetic disturbance duration is tentatively defined as the length of the time interval in which the H-component geomagnetic deviation exceeds half of the maximum deviation from the beginning of main phase. The results given in Figs. 49 and 53 suggest the close association of the hiss with ring-current particles. Moreover, the close correlation of the hiss with the geomagnetic activity shown in Figs. 48 and 53 seems to suggest that a favorable condition required for the hiss generation is not satisfied until the quantity of ring-current particles exceeds a 'threshold level'.

Taking into account the close association of storm-time hiss with the phase of storms, an examination is made of the time lag of occurrence of hiss behind the time of maximum depression in geomagnetic field. The time of maximum hiss intensity is delayed considerably behind the time of maximum deviation of the geomagnetic H component. Considering that the DR field is mainly attributable to the drift of quasi-trapped protons and electrons of the order of 100 keV, and taking account the longitudinal dependence of the drift velocity on the kinetic energy of charged particles (HAMLIN *et al.*, 1961), the considerable delay time of hiss occurrence could be explained by an

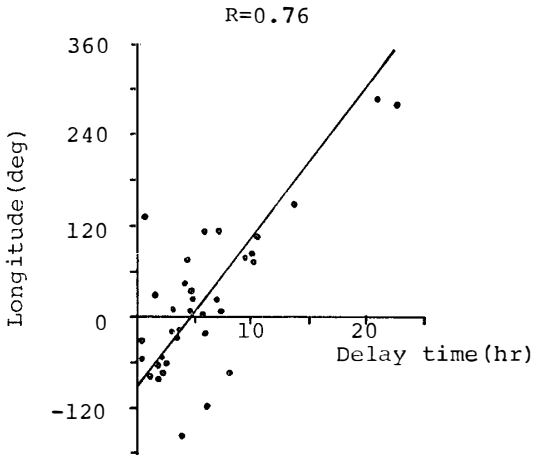

Fig. 54. Time delay of the maximum intensity of hiss behind the maximum H-depression of geomagnetic field versus the longitude (measured eastward from the midnight meridian) of the local time of maximum hiss intensity. The regression line is also indicated.

overwhelming contribution from low-energy particles. Fig. 54 illustrates the longitude (measured eastward from the midnight meridian) of occurrence of hiss versus the delay time. Using a linear least-squares fit, the relation between the longitude and the delay time is found to be

$$\text{Longitude(deg)} = 20\text{(deg/hr)} \times \text{Delay time(hr)} - 90\text{(deg)}$$

Hence, it is suggested that storm-time hiss is associated with soft electrons injected into the evening sector of the magnetosphere during and after the main phase, and rotating eastward at a drift velocity of 20 deg / hr. Assuming co-rotation of the ring current region with the Earth (at 15 deg / hr) and longitudinal drift of charged particles in the equatorial plane at ~ 3 Re due to the gradient and curvature of the geomagnetic field, the energy of electrons drifting at 5 deg / hr is estimated to be of order $\sim$ 5keV (TANAKA *et al.*, 1974). In this paper a clear understanding has been obtained concerning the distinction of morphological properties between auroral hiss and low-latitude VLF hiss. The generation as well as propagation mechanisms of auroral and low-latitude hiss have not been well understood and further observational and theoretical investigation should be made.

5. Concluding Remarks

The DF system described in this paper is found to be very effective for isolated and sharp VLF bursts, but this system does not provide us with accurate information on the incident and azimuthal angles for the noise-like VLF hiss. So, we have to develop a new DF system which is more effective and accurate for noise-like emissions than the DF system based on the analysis of Lissajous' figures of electromagnetic fields. This system being planned is described in 4.3. in Part I.

It has recently been accepted that auroral hiss is generated by the incoherent Cerenkov mechanism, but the theoretical value of its intensity is still lower than the observed value. Therefore, we must study in more detail the generation region of auroral hiss and the most important problem in its generation mechanism, whether the plasma instability is involved or not, by observing accurately the position of the exit point as well as the wave coherency with our newly developed system.

Low-latitude VLF hiss is found in Part II to be an essentially different phenomenon from auroral hiss. This point will be further examined by simultaneous observations at the auroral zone and at low-latitude stations such as Moshiri. Our idea that the low-latitude VLF hiss during storm-time may be generated by soft ring-current electrons on the order of ~ 5 keV, is to be studied by making use of simultaneous ground-based observations on a world-wide scale as well as *in-situ* observations by rockets and satellites.

References

AKASOFU, S.-I. (1968): Polar and Magnetospheric Substorms. D. Reidel, Dordrecht, 140-154.

BANKS, P. (1966): Collision frequencies and energy transfer. Planet. Space Sci., **14**, 1105-1122.

BULLOUGH, K., and J. L. SAGREDO (1973): VLF goniometer observations at Halley Bay, Antarctica—I. The equipment and the measurement of signal bearing. Planet. Space Sci., **21**, 899-912.

BULLOUGH, K., A.R.W. HUGHES, and T.R. KAISER (1969a): VLF observations on Ariel 3. Proc. R. Soc. London, **A311**, 563-569.

BULLOUGH, K., A. R. W. HUGHES, and T. R. KAISER (1969b): Satellite evidence for the generation of VLF emissions at medium latitudes by the transverse resonance instability. Planet. Space Sci., **17**, 363-374.

BULLOUGH, K., A.R.W. HUGHES, and T.R. KAISER (1974): Spacecraft studies of VLF emissions. Magnetospheric Processes, ed. by B.M. MCCORMAC, D. Reidel, Dordrecht, 231-240.

BURTIS, W.J. (1969): Magnetic radiation observed by the Ogo 1 and Ogo 3 broadband VLF receivers. Tech. Rep., Radioscience Lab., Stanford Univ., Stanford, Calif., **3438-1**.

CARTWRIGHT, D.G. (1960): Direction-finding on diffuse sources of electromagnetic radiation. Aust. J. Phys., **13**, 712-717.

COLE, R.K., and E.T. PIERCE (1965): Electrification in the earth's atmosphere for altitudes between 0 and 100 kilometers. J. Geophys. Res., **70**, 2735-2749.

COUSINS, M.D. (1972): Direction finding on whistlers and related VLF signals. Radioscience Lab., Stanford Univ., Stanford, Calif., SEL-72-013.

DELLOUS, J., and M. GARNIER (1963): Sur l'émergence des sifflements radio-électriques hors de l'ionosphère. C. R. Acad. Sci., **257**, 1327-1330.

DOWDEN, R.L. (1960): Geomagnetic noise at 230 kHz. Nature, **187**, 677-678.

ECKLUND, W.L., J.K. HARGREAVES, and J.H. POLE (1965): On the relation between auroral radio absorption and very low frequency emissions. J. Geophys. Res., **70**, 4285-4292.

ELLIS, G.R.A. (1959): Low frequency electromagnetic radiation associated with magnetic disturbances. Planet. Space Sci., **1**, 253-258.

FRITZ, T.A., and D.A. GURNETT (1965): Diurnal and latitudinal effects observed for 10-kev electrons at low satellite altitudes. J. Geophys. Res., **70**, 2485-2502.

GURNETT, D.A. (1966): A satellite study of VLF hiss. J. Geophys. Res., **71**, 5599-5615.

GURNETT, D.A. (1968): Observation of VLF hiss at very low L values. J. Geophys. Res., **73**, 1096-1101.

GURNETT, D.A., and L.A. FRANK (1972): VLF hiss and related plasma observations in the polar magnetosphere. J. Geophys. Res., **77**, 172-190.

HAMLIN, D.A., R. KARPLUS, R.C. VIK, and K.M. WATSON (1961): Mirror and azimuthal drift frequencies for geomagnetically trapped particles. J. Geophys. Res., **66**, 1-4.

HARANG, L. (1968): VLF emission observed at stations close to the auroral zone and at stations on lower latitudes. J. Atmos. Terr. Phys., **30**, 1143-1160.

HARANG, L., and R. LARSEN (1965): Radio wave emissions in the VLF band observed near the auroral zone, I. Occurrence of emissions during disturbances. J. Atmos. Terr. Phys., **27**, 481-497.

HARANG, L., and K.N. HAUGE (1965): Radio wave emissions in the VLF band observed near the auroral zone, II. Physical properties of the emissions. J. Atmos. Terr. Phys., **27**, 499-512.

HARTZ, T.R., and N.M. BRICE (1967): The general pattern of auroral particle precipitation. Planet. Space Sci., **15**, 301-329.

HAYAKAWA, M., and J., OHTSU (1972): Transmission and reflection of magnetospheric whistlers in the lower exosphere and ionosphere at high latitudes. Planet. Space Sci., **20**, 1895-1907.

HAYAKAWA, M., Y. TANAKA, and J. OHTSU (1975): The morphologies of low-latitude and auroral VLF 'hiss'. J. Atmos. Terr. Phys., **37**, 517-529.

HAYAKAWA, M., Y. TANAKA, and J. OHTSU (1975): Satellite and ground observations of magnetospheric VLF hiss associated with the severe magnetic storm on May 25-27, 1967. J. Geophys. Res., **80**, 86-92.

HELMS, W.J., and J.P. TURTLE (1964): A cooperative report on the correlation between aurorae, magnetic, and ELF phenomena at Byrd Station. Tech. Rep., Radioscience Lab., Stanford Univ., Stanford, Calif., **3408**.

HOLT, O., and A. OMHOLT (1962): Auroral luminosity and absorption of cosmic noise. J. Atmos. Terr. Phys., **24**, 467-474.

HUGHES, A.R.W., and T.R. KAISER (1971): VLF radio emissions and aurora. Radiating Atmosphere, ed. by B.M. MCCORMAC, D. Reidel, Dordrecht, 336-344.

IWAI, A. (1962): Study of the observational method of atmospherics and whistlers. Doctoral Thesis, Nagoya Univ.

IWAI, A., and Y. TANAKA (1968): Measurement of polarization, incident angle and direction of VLF emissions-(I). Proc. Res. Inst. Atmos., Nagoya Univ., **15**, 1-16.

IWAI, A., J. OUTSU, and Y. TANAKA (1964): The observation of VLF emissions at Moshiri. Proc. Res. Inst. Atmos., Nagoya Univ., **11**, 29-40.

JAMES, H.G. (1973): Whistler mode hiss at low and medium frequencies in the day side cusp ionosphere. J. Geophys. Res., **78**, 4578-4599.

JESPERSEN, M., A. HAUG, and B. LANDMARK (1966): Electron density and collision frequency observations in the arctic D-region. Electron Density Profiles in Ionosphere and Exosphere, ed. by J. Frihagen, North-Holland, Amsterdam, 27-30.

JØRGENSEN, T.S. (1966): Morphology of VLF hiss zones and their correlation with particle precipitation events. J. Geophys. Res., **71**, 1367-1375.

JØRGENSEN, T.S. (1968): Interpretation of auroral hiss measured on Ogo 2 and at Byrd Station in terms of incoherent Cerenkov radiation. J. Geophys. Res., **73**, 1055-1069.

KAISER, T.R. (1972): VLF phenomena. Earth's Magnetospheric Processes, ed. by B. M. MCCORMAC, D. REIDEL, Dordrecht, Holland, 340-350.

KNUDSEN, W.G. (1968): Equatorial VLF hiss and intense fluxes of soft electrons. J. Geophys. Res., **73**, 6384-6386.

KUCK, G.A. (1970): Local time dependence of aurora zone electron spectra. Ann. Geophys., **26**, 689-695.

LAASPERE, T., and W.C. JOHNSON (1973): Additional results from an Ogo 6 experiment concerning ionospheric electric and electromagnetic fields in the range 20 Hz to 540 kHz. J. Geophys. Res., **78**, 2926-2944.

LAASPERE, T., M.G. MORGAN, and W.C. JOHNSON (1964): Chorus, hiss and other audio-frequency emissions at stations of the Whistler-East network. Proc. IEEE, **52**, 1331-1349.

LAASPERE, T., W.C. JOHNSON, and L.C. SEMPREBON (1971): Observations of auroral hiss, LHR noise, and other phenomena in the frequency range 20 Hz to 540 kHz on Ogo 6. J. Geophys. Res., **76**, 4477-4493.

LIKHTER, YA. I., V.I. LARKINA, and YU. M. MIKHALOV (1973): Presented at COSPAR meeting, Konstantz, FRG.

LIM, T.L., and T. LAASPERE (1972): An evaluation of the intensity of Cerenkov radiation from auroral electrons with energies down to 100 ev. J. Geophys. Res., **77**, 4145–4157.

MAEDA, K., and I. KIMURA (1956): A theoretical investigation on the propagation path of the whistling atmospherics. Rep. Ionos. Res. Japan, **5**, 105–123.

MARTIN, L.H., R.A. HELLIWELL, and K.E. MARKS (1960): Association between aurorae and VLF hiss observed at Byrd Station, Antarctica. Nature, **187**, 751–753.

MCEWEN, D.J., and R.E. BARRINGTON (1967): Some characteristics of the lower hybrid noise bands observed by the Alouette I satellite. Can. J. Phys., **45**, 13–20.

MIYAZAKI, S. (1975): Results of rocket observation of electron density at Syowa Station. Antarct. Rec., **52**, 128–140.

MOROZUMI, H.M., and R.A. HELLIWELL (1966): A correlating study of the diurnal variation of upper atmospheric phenomena in the southern auroral zone. Sci. Rep. Radiosci. Lab., Stanford Univ., **2**.

MOSIER, S.R., and D.A. GURNETT (1969): VLF measurement of the Poynting flux along the geomagnetic field with the Injun 5 satellite. J. Geophys. Res., **74**, 5675–5687.

NISHINO, M., and Y. TANAKA (1969a): Occurrence of VLF emissions at Syowa Station. Antarct. Rec., **35**, 37–51.

NISHINO, M., and Y. TANAKA (1969b): Polarization and arriving direction of VLF emissions. JARE Sci. Rep., Ser. A, **7**, 14 pp.

ONDOH, T. (1963): The ionospheric absorption of the VLF emissions at the auroral zone. J. Geomag. Geoelect., **15**, 90–108.

OUTSU, J., Y. TANAKA, and A. IWAI (1963): Annual variation of whistler occurrence rate in middle and low latitudes since July 1957. Bull. Res. Inst. Atmos., Nagoya Univ., **13**, 11–24.

PAULIKAS, G.A. (1971): The patterns and sources of high-latitude particle precipitation. Rev. Geophys. Space Phys., **9**, 659–701.

RAO, M., V.V. SOMAYAJULU, and B.A.P. TANTRY (1972): An analysis of multi-station ground observations of VLF hiss. J. Geomag. Geoelect., **24**, 261–265.

RUSSELL, C.T., R.L. MCPHERRON, and P.J. COLEMAN (1972): Fluctuating magnetic field in the magnetosphere 1 : ELF and VLF fluctuations. Space Sci. Rev., **12**, 810–856.

TANAKA, Y. (1972): VLF hiss observed at Syowa Station, Antarctica. I-Observation of VLF hiss, II-Occurrence and polarization of VLF hiss during disturbances. Proc. Res. Inst. Atmos., Nagoya Univ., **19**, 33–94.

TANAKA, Y., and M. KASHIWAGI (1968): Correlation between VLF hiss and geomagnetic activity in Hokkaido. Proc. Res. Inst. Atmos., Nagoya Univ., **15**, 67–73.

TANAKA, Y., M. NISHINO, and A. IWAI (1970): VLF hiss at Syowa Station. Proc. Res. Inst. Atmos., Nagoya Univ., **18**, 43–56.

TANAKA, Y., M. HAYAKAWA, and J. OHTSU (1974): VLF hiss observed at a low-latitude ground station and its relation to drifting ring current electrons. Rep. Ionos. Space Res. Japan, **28**, 168–172.

TAYLOR, W.W.L., and S.D. SHAWHAN (1974): A test of incoherent Cerenkov radiation for VLF hiss and other magnetospheric emissions. J. Geophys. Res., **89**, 105–117.

THOMAS, L. (1969): The effects of ions on the propagation of e. l. f. and v. l. f. waves in the lower ionosphere. J. Atmos. Terr. Phys., **31**, 991–1002.

THOMAS, L., and J.R. SMEATHERS (1971): The internal reflection of whistler waves in the lower ionosphere. J. Atmos. Terr. Phys., **33**, 959–962.

TSURUDA, K., and K. HAYASHI (1975): Direction finding technique for elliptically polarized VLF electromagnetic waves and its application to the low-latitude whistlers. J. Atmos. Terr. Phys., **39**, 1193–1202.

TULUNAY, Y.K., and A.R.W. HUGHES (1973): A satellite study of the mid-latitude trough in electron density and VLF radio emissions during the magnetic storm of 25-27 May, 1967. J. Atmos. Terr. Phys., **35**, 153-163.

VERSHININ, E.F. (1970): About the intensity of the hiss near inner boundary of the plasmapause and about the bursts of hiss with drifting frequency. Ann. Géophys., **26**, 703-707.

(*Manuscript received September 9, 1975*)